Title: **Systematic mapping of small nucleolar RNA targets in human cells**

Authors: Hywel Dunn-Davies[1*], Tatiana Dudnakova[1*], Jean-Louis Langhendries[2], Nicholas Watkins[3], Denis L.J. Lafontaine[2] and David Tollervey[1,4]

* These authors contributed equally

Affiliations:

1 Wellcome Centre for Cell Biology, University of Edinburgh, Michael Swann Building, King's Buildings, Mayfield Road, Edinburgh EH9 3BF, Scotland

2 RNA Molecular Biology, Fonds de le Recherche Scientifique (F.R.S./FNRS), Université Libre de Bruxelles (ULB), Belgium

3 Institute for Cell and Molecular Biosciences, Newcastle University, Newcastle upon Tyne, UK

4 Correspondence to: d.tollervey@ed.ac.uk

Running title: Mapping snoRNA targets

Key words: small nucleolar RNA, snoRNA, RNA-RNA interaction, RNA-protein interaction, UV cross-linking, methylation, RNA modification, epitranscriptomics

ABSTRACT

Altered expression of box C/D small nucleolar RNAs (snoRNAs) is implicated in human diseases, including cancer. Box C/D snoRNAs canonically direct site-specific, 2'-*O*-methylation but the extent to which they participate in other functions remains unclear. To identify RNA targets of box C/D snoRNAs in human cells, we applied two techniques based on UV crosslinking, proximity ligation and sequencing of RNA hybrids (CLASH and FLASH). These identified hundreds of novel snoRNA interactions with rRNA, snoRNAs and mRNAs. We developed an informatic pipeline to rigorously call interactions predicted to direct methylation. Multiple snoRNA-rRNA interactions identified were not predicted to direct RNA methylation. These potentially modulate methylation efficiency and/or contribute to folding dynamics. snoRNA-mRNA hybrids included 1,300 interactions between 117 snoRNA families and 940 mRNAs. Human U3 is substantially more abundant than other snoRNAs and represented about 50% of snoRNA-mRNA hybrids. The distribution of U3 interactions across mRNAs also differed from other snoRNAs. Following U3 depletion, mRNAs showing altered abundance were strongly enriched for U3 CLASH targets. Most human snoRNAs are excised from pre-mRNA introns. Enrichment for snoRNA association with branch point regions of introns that contain snoRNA genes was common, suggesting widespread regulation of snoRNA maturation.

INTRODUCTION

The small nucleolar RNAs (snoRNAs) are a class of abundant, small stable RNAs, most of which act as guides for site-specific RNA modification. Most members of the box C/D class of snoRNAs select sites of ribose 2'-*O*-methylation by extended regions of perfect complementarity with target sites (≥12 bp), in which the nucleotide to be modified is placed exactly 5 bp from the conserved box D or box D' motifs within the snoRNA (reviewed in (Tollervey and Kiss, 1997; Watkins and Bohnsack, 2012)). The box C/D snoRNAs associate with a group of four common proteins, NOP56, NOP58, 15.5K and the methyltransferase Fibrillarin. The snoRNAs have a partially symmetrical structure, in which stem structures bring together the highly conserved, terminal box C (RUGAUGA, R = A or G) and box D (CUGA) sequences and the related, but less conserved, internal box C' and box D' elements. These stem structures include a K-turn structural motif that is bound by the small 15.5K protein. *In vitro* structural analysis indicated that the box C/D stem is also bound by NOP58, while the box C'/D' stem is bound by the homologous NOP56 protein. Each region is bound by a copy of NOP1, so the regions flanking either box D, box D' or both can function as methylation guides. In human cells, snoRNA-

directed methylation sites show variable stoichiometry, indicating regulation that is likely to be functionally important (reviewed in (Henras et al., 2017; Sloan et al., 2017)).

The strict requirement for a long region of perfect complementarity that extends to box D/D' for guide function implies that strong snoRNA base pairing could occur without eliciting target RNA methylation. Indeed, a small number of box C/D snoRNAs have essential functions in ribosome synthesis that require snoRNA/pre-rRNA base pairing without associated rRNA methylation. In vertebrates, these snoRNAs include U3, U14 and U8 (reviewed in (Watkins and Bohnsack, 2012)). In addition, pre-rRNA base-pairing by U13 snoRNA directs formation of N^4-acetyl cytidine (ac4C) by NAT10, rather than methylation (Sharma et al., 2015; Sharma et al., 2017b).

Other acetylation targets are not known, but human snoRNAs can direct methylation of small RNAs, including spliceosomal small nuclear RNAs (snRNAs) and other snoRNAs (Bouchard-Bourelle et al., 2019; Bouchard-Bourelle et al., 2020; Dupuis-Sandoval et al., 2015). A number of human snoRNAs have been reported to bind mRNAs, with effects on pre-mRNA splicing and 3' end formation (Falaleeva et al., 2016; Huang et al., 2017). Human snoRNAs show tissue-specific expression patterns, with altered expression linked to disease and tumorigenesis (Bergeron et al., 2021; Bratkovič et al., 2020; Fafard-Couture et al., 2021; Siprashvili et al., 2016; Su et al., 2013; Thorenoor and Slaby, 2015; Xu et al., 2014; Zhou et al., 2017). The imprinted, brain-specific snoRNAs snoRD115 and snoRD116 are implicated in the neurological disease Prader-Willi syndrome [see (Bieth et al., 2015; Burnett et al., 2017; Falaleeva et al., 2016; Falaleeva et al., 2015; Rozhdestvensky et al., 2016) reviewed in (Cavaillé, 2017)]. Mutations in U8/snoRD118 cause the neurological disease leukoencephalopathy with calcification and cysts in humans (Frenk et al., 2014) and a Zebrafish model (Badrock et al., 2020). In addition, snoRNAs can apparently function by direct protein binding: Loss of specific snoRNAs reduced levels of the GTP-bound, active form of K-Ras with consequent hyperactivation of the Ras-ERK1/ERK2 signaling pathway (Siprashvili et al., 2016). snoRNAs were also implicated in activation of the immune regulator Protein Kinase RNA-activated (PKR) under conditions of metabolic stress (Youssef et al., 2015).

Bioinformatics approaches have been used to predict snoRNA binding sites in several systems, particularly where this is associated with methylation (Jorjani et al., 2016; Lowe and Eddy, 1999; Lu et al., 2016; Omer et al., 2000). In addition, a number of recent reports have described methods for the identification of RNA-RNA interactions through proximity ligation followed by

sequencing of the products of reverse transcription and PCR amplification (RT-PCR) (Bharathavikru et al., 2017; Dudnakova et al., 2018; Kudla et al., 2011; Sharma et al., 2016; Sugimoto et al., 2015). The crosslinking and sequencing of hybrids (CLASH) approach used stringent tandem affinity purification including denaturing conditions to recover RNA-protein and RNA-RNA interactions involving yeast snoRNAs (Dudnakova et al., 2018; Kudla et al., 2011) and human miRNAs (Helwak et al., 2013; Helwak and Tollervey, 2014). A related approach, formaldehyde-assisted crosslinking and sequencing of hybrids (FLASH) combines immunoprecipitation with mild chemical crosslinking, which stabilizes protein complexes allowing denaturing wash conditions (Bharathavikru et al., 2017). Here we report the use of CLASH and FLASH to systematically map the interactions between box C/D snoRNAs and the human transcriptome.

MATERIALS AND METHODS

Human cell culture and UV crosslinking

Human embryonic kidney HEK cells were gown to 80% confluency in DMEM, 10%FBS medium and were UV crosslinked on ice with λ = 254 nm in Stratalinker 1800 (Stratagene), at 400 mJ/cm2. U3 was depleted from HEK cells by use of a chimeric antisense oligonucleotide, as described (Langhendries et al., 2016).

HEK Cell Lysis

HEK cells were lysed by addition of ice-cold TM150 buffer (20 mM Tris-HCl pH 7.4, 150 mM NaCl, 0.4% NP-40, 2mM MgCl2, 1 mM DTT, protease inhibitors (Roche, complete, EDTA-free), RNAse Inhybitor (Promega)). 10u of RQ1DNAse (Promega) were added, the samples were mixed by pipetting and incubated for 10 min at room temperature to break genomic DNA and to ease the extraction of nuclear Fibrillarin binding complexes. Lysates were centrifuged in Eppendorf mini centrifuge at 14000rpm and 4C for 10 min and supernatant was collected.

First affinity purification

In human HEK CLASH beads conjugated with anti-Flag M2 (Sigma), in FLASH Protein A agarose conjugated with IgG and anti-FBL AB were used. Cell lysates were incubated with beads for 60 min at 4°C. Supernatant was discarded and the recovered beads were washed twice with PBS-WB buffer (PBS, plus 150mM NaCl, 2 mM MgCl2, 0.4% NP-40), and once in 1X PBS, 2mM MgCl2.

4

RNase treatment and formaldehyde crosslinking

RNP complexes bound to the beads were treated with 0.5 unit RNaseA+T1 mix (RNace-IT, Stratagene) in 100 µl PBS,2mM MgCl2 buffer for 10 min at 20°C. In CLASH 900 µl GDB denaturing buffer (6M GuCl2, 150mM NaCl, 20mM Tris pH=7.4) was added to the beads with RNase and mixed thoroughly. Supernatant with denatured complexes was removed and added to Ni beads (Gibco) washed in GDB, subsequent binding carried out for 1h at 4C. In FLASH to remove indirect RNA and protein binding from the complexes the beads were washed twice with PBS-WB buffer (PBS, +150mM NaCl, 2 mM MgCl2, 0.4% NP-40), twice with HS-PBS-WB (PBS, 0.3 M NaCl, 2 mM MgCl2, 0.4% NP-40) and once in 1xPBS. The complexes were cross linked on beads in 0.2% formaldehyde in PBS for 3 min, then formaldehyde was quenched by addition of glycine to 0.2M and Tris-HCl pH=8 to 0.1M and incubation for 5 min. Crosslinked complexes were subjected to 4x denaturing washes in UB (20 mM Tris pH=7.4, 8M UREA, 0.3M NaCl, 0.4% NP-40) and additional incubation in UB for 30 min at 4C to remove nonspecific interactions. Subsequent steps were identical for FLASH and CLASH.

RNA end modification

In CLASH Ni beads were washed twice with GDB buffer, twice with TM150, twice with PNK buffer (50 mM Tris-HCl pH 7.5, 10 mM MgCl$_2$, 0.5% NP-40, 50 mM NaCl).
In FLASH beads with bound RNA-protein complexes were washed 4x with PNK buffer.
To remove unwanted 3'phosphate groups from bound RNA fragments in both CLASH and FLASH the complexes were treated with TSAP phosphatase (Promega) using provided buffer for 40 min at room temperature. To inactivate the enzyme the beads were washed twice with UB (FLASH) or GDB (CLASH) and 4x with PNK buffer.
Then the 5' phosphorylation and radioactive labelling of RNA was carried out. The complexes on the beads were incubated with 40 units T4 Polynucleotide kinase (New England Biolabs), first with P32 labelled ATP for 45 min, then 20 more min with 1 mM cold ATP, in PNK buffer with RNase inhibitors (RNasin, Promega) at room temperature. The reaction should provide 5' phosphates needed for downstream ligations. The beads then were washed as before twice UB (FLASH) or GDB (CLASH) and 4x PNK buffer.

Linker ligation and RNA-protein complex elution

Protein-bound RNA molecules were ligated together and with 3' linker (1 µM miRCat-33, IDT), overnight using 40 units of T4 RNA ligase 1 (New England Biolabs) in PNK buffer with RNase

5

inhibitors at 16°C. This reaction created RNA hybrids and single RNA molecules ligated to miRCat linker. On the next day, the beads were washed as before 2x UB (FLASH) or GDB (CLASH) and 4x PNK buffer. Then using 40 units of RNA ligase 1, barcoded 5′ linkers (final conc. 5 μM; IDT, one for each sample) were ligated in RNA ligase 1 buffer with 1mM ATP for 3-6 h at 20°C. The beads were washed as before. In CLASH the complexes were eluted in EB (2x NuPage Sample buffer, 400 mM Imidazole, 10mM Tris-HCl pH=7.4, 10mM DTT). In FLASH the complexes were washed off the beads by partial destruction of formaldehyde crosslinking by boiling the samples in NuPAGE protein sample buffer plus 100 mM Tris-HCl, 1%SDS, 100 mM ME (β-mercaptoethanol) for 3 min. The supernatant with RNA-protein complexes was recovered from cooled samples.

SDS-PAGE, and transfer to nitrocellulose

Protein-RNA complexes in NuPAGE SB plus SDS, ME (Life Technologies) were resolved on a 4%–12% Bis-Tris NuPAGE gel (Life Technologies) in NuPAGE SDS MOPS running buffer then they were transferred to nitrocellulose membrane (GE Healthcare, Amersham Hybond ECL) in NuPage transfer buffer (Life Technologies) with 10% methanol for 1 hr at 100V. Depending on the strength of the signal the membrane was exposed on film (Amersham) for 1 hr or overnight at -70C. Developed film was aligned with the membrane and the radioactive bands corresponding to the Fibrillarin-RNA complexes were excised.

Proteinase K Treatment, RNA Isolation and cDNA Library preparation

Cut out bands were incubated with 150 μg of Proteinase K (Roche) and proteinase K buffer (50 mM Tris-HCl pH 7.8, 50 mM NaCl, 0.4% NP-40, 0.5% SDS, 5 mM EDTA) for 2 hr at 55°C. The RNA was extracted with phenol-chloroform-isoamyl alcohol (PCI) mixture and ethanol precipitated overnight with 10 μg Glycogen (Ambion, Life Technologies). The isolated RNA was dissolved in 12 mkL of distilled RNAse-free water and reverse transcribed using miRCat-33 primer (IDT) with Superscript III Reverse Transcriptase (Life Technologies) in its buffer for 1h at 50°C. RNA was then degraded by addition of RNase H (New England Biolabs) for 30 min at 37°C. cDNA was amplified using primers P5 and primer PE_miRCat_PCR and TaKaRa LA Taq polymerase (Takara Bio). PCR products were separated on a 2% MetaPhor agarose (Lonza) gel with SYBRSafe (Life Technologies) in 1 x TBE at +4C. The gel band corresponding to 150-200bp was cut out. cDNA was purified with MinElute Gel Extraction Kit (QIAGEN). Obtained cDNA libraries were sent for high-throughput sequencing.

Oligonucleotides

3' linker

miRCat-33 linker (IDT) AppTGGAATTCTCGGGTGCCAAG/ddC/

5' linkers

L5Aa invddT-ACACrGrArCrGrCrUrCrUrUrCrCrGrArUrCrUrNrNrN<u>rUrArArGrC</u>-OH L5Ab invddT-ACACrGrArCrGrCrUrCrUrUrCrCrGrArUrCrUrNrNrN<u>rArUrUrArGrC</u>-OH

L5Ac invddT-ACACrGrArCrGrCrUrCrUrUrCrCrGrArUrCrUrNrNrN<u>rGrCrGrCrArGrC</u>-OH

L5Bb invddT-ACACrGrArCrGrCrUrCrUrUrCrCrGrArUrCrUrNrNrN<u>rGrUrGrArGrC</u>-OH

L5Bc invddT-ACACrGrArCrGrCrUrCrUrUrCrCrGrArUrCrUrNrNrN<u>rCrArCrUrArGrC</u>-OH

L5Bd invddT-ACACrGrArCrGrCrUrCrUrUrCrCrGrArUrCrUrNrNrN<u>rUrCrUrCrUrArGrC</u>-OH

L5Ca invddT-ACACrGrArCrGrCrUrCrUrUrCrCrGrArUrCrUrNrNrN<u>rCrUrArGrC</u>-OH

L5Cb invddT-ACACrGrArCrGrCrUrCrUrUrCrCrGrArUrCrUrNrNrN<u>rGrGrArGrC</u>-OH

L5Cc invddT-ACACrGrArCrGrCrUrCrUrUrCrCrGrArUrCrUrNrNrN<u>rArCrTrCrArGrC</u>-OH

L5Cd invddT-ACACrGrArCrGrCrUrCrUrUrCrCrGrArUrCrUrNrNrN<u>rGrArCrTrTrArGrC</u>-OH

The fixed barcodes are underlined. N indicates mixed nucleotides for random barcodes.

PCR primers

miRCat-33 primer (IDT) CCTTGGCACCCGAGAATT primer for RT

PE_miRCat_PCR

CAAGCAGAAGACGGCATACGAGATCGGTCTCGGCATTCCTGGCCTTGGCACCCGAGAATT

CC library amplification

P5 AATGATACGGCGACCACCGAGATCTACACTCTTTCCCTACACGACGCTCTTCCGATCT

library amplification

Bioinformatics

Analysis of CLASH data

Raw sequences were preprocessed prior to alignment using hyb (Travis et al., 2014) by running the hyb preprocess command with standard parameters. The preprocessed data were aligned to a custom database combining multi-exon transcripts and unspliced genes (with snoRNA genes extended by 20bps in each direction and masked out of the genes in which they are contained where appropriate). The custom database was built using reference data from Ensembl release 77 (www.ensembl.org). To facilitate the analysis of snoRNA/rRNA hybrids, the complete human ribosomal DNA repeating unit (https://www.ncbi.nlm.nih.gov/nuccore/U13369) was also included

7

in the database. Sequence alignment was performed using the blastall command, using the standard parameters from the hyb pipeline (Travis et al., 2014). The aligned reads were processed using a variant of the hyb pipeline, modified slightly to extract snoRNA hybrids rather than microRNA hybrids preferentially. Hybrids identified using this process were then filtered to exclude sequences that could be aligned as single reads to the human genome (Ensembl release 77) using Novoalign 2.07 (www.novocraft.com) to prevent single reads overlapping gene boundaries from being mistakenly identified as hybrids. Downstream analysis was performed on reproducible hybrids (in which both fragments were found to overlap in two or more hybrids) with a predicted folding energy of -12dG or below. Among these stable, reproducible hybrids, further filters were applied to ensure that hybrids between snoRNAs and other classes of RNA were not mismapped U3 stems, and that hybrids between snoRNAs and RNAs that were not snoRNAs or rRNAs were not mismapped snoRNA-rRNA hybrids. The analysis was performed using the hybtools python package (http://www.github.com/hyweldd/hybtools), which was developed for this project. Reference data for the analysis of human methylation sites were obtained from (Krogh et al., 2016) and (Jorjani et al., 2016).

All interactions recovered are listed in Dataset 1.

Analysis of RNA-Seq data

RNA-Seq data were processed using STAR (Dobin et al., 2013) and DESeq2 (Love et al., 2014), using a human genome database from ensemble release 77 (www.ensembl.org).

RESULTS

Systematic mapping of box C/D snoRNA interactions by UV crosslinking

To identify potential novel snoRNA interactions we initially applied the CLASH technique (Figure 1A) (Helwak et al., 2013; Kudla et al., 2011). This involves UV crosslinking of RNA complexes with tagged proteins in living cells and affinity purification of the RNP complexes under stringent conditions. Ligation of linker adaptors is performed in parallel with internal ligation of captured RNA fragments base paired to each other. RNA is isolated, including RNA hybrids, followed by reverse transcription and high throughput sequencing of cDNA libraries.

CLASH analyses require the use of a "bait" protein fused to a tandem affinity purification tag. For these analyses, we tagged the core box C/D snoRNP proteins Fibrillarin (FBL) or NOP56 with a

C-terminal tag consisting of His6 – Precision protease cleavage site – Flag epitope. Tagged constructs were integrated into the chromosome in Flip-in HEK293 cells at a pre-inserted LoxP site. The fusion proteins were expressed under a regulated pCMV-2xTET O_2 promoter. Tetracyclin levels were titrated to achieve expression close to the endogenous protein level, as assessed by western blotting. The tagged proteins were previously shown to be functional in rRNA processing by rescue experiments, in which the endogenous proteins were depleted by RNAi (Knox et al., 2011).

In order to assess robustness of our dataset we performed orthogonal validation, using formaldehyde assisted crosslinking ligation and sequencing of hybrids (FLASH) (Bharathavikru et al., 2017). This approach is similar to CLASH in that RNA-protein interactions are captured by UV crosslinking in growing cells, but antibodies are used for affinity purification of endogenous RNA-protein complexes. During purification, brief formaldehyde crosslinking is used to stabilize binding of the covalent bait protein-RNA complex to the protein A beads, allowing column washes under highly denaturing conditions. Analyses of single hits for FBL and NOP56 showed that, for both proteins, snoRNA sites were most frequently recovered followed by rRNA and then mRNA hits, in both CLASH and FLASH analyses (Supplementary Figure 1), supporting the reliability of the crosslinking approaches.

In human cells we recovered 591,958 hybrids overall (Supplementary Figure 2A; Table S1; Dataset 1). Recovered sequences that could be confidently mapped to two distinct regions of the genome (see Methods) were regarded as representing chimeric cDNAs resulting from RNA-RNA ligation. Non-identical chimeric sequences, or sequences recovered from different analyses, in which both segments overlapped were regarded as demonstrating independent recovery of the same interaction. The recovered RNA sequences were folded *in silico,* using the ViennaRNA Package 2.0 (Lorenz et al., 2011), to assess whether they arose from a stable RNA-RNA duplex. Interactions supported by at least two independent sequences, with a predicted ΔG of less than -12 Kcal mol^{-1}, were considered stable and reproducible, and included in further analyses; this was the case for a total of 449,781 hybrids (Supplementary Figure 2A). Among stable, reproducible hybrids, further filters were applied to ensure that hybrids called between snoRNAs and other classes of RNA were not mismapped internal snoRNA stems, and that hybrids between snoRNAs and RNAs that were not snoRNAs or rRNAs were not mismapped snoRNA-rRNA hybrids.

9

We compared CLASH from the cells expressing tagged Fibrillarin with FLASH from untagged control cells using anti-Fibrillarin antibodies. Strikingly, 97% of stable, reproducible RNA-RNA interactions recovered by CLASH were mapped to sites of interactions also recovered in FLASH: (Figure 1B). A lower fraction of hybrids recovered by FLASH corresponded to interaction sites also found in CLASH data (66% of hybrids), with 34% FLASH only hybrids (Figure 1B).

The majority of hybrids mapping to snoRNAs were internal, representing stem structures (Supplementary Figure 2; Table S1). These potentially allow visualization and analysis of snoRNA structures. Among intermolecular snoRNA hybrids, snoRNA-rRNA hybrids were most frequently recovered. From the set of stable, reproducible intermolecular hybrids after filtering, 69% were snoRNA-rRNA interactions, 9% were snoRNA-mRNA interactions, and 17% were snoRNA-snoRNA. It is notable that some highly abundant RNA species were recovered at low levels, in particular snoRNA-tRNA interactions represented only 0.7% of intermolecular hybrids, supporting the specificity of the interactions. The predominant recovery of snoRNA-rRNA interactions is consistent with the known function of snoRNAs in ribosome synthesis. Recovery of different RNA species in single reads (Supplementary Figure1) and chimeras (Supplementary Figure 2) was in general agreement, supporting the recovery of authentic interactions.

To confirm the reliability of both methods we compared snoRNA-rRNA interactions recovered as hybrids in both types of experiments with the position of known rRNA methylation sites (Figure 1C). Comparing CLASH and FLASH results for snoRNA-rRNA targeting in human HEK cells we noticed that although peak intensities varied to some extent, the same major interactions were recovered with both methods and correlated with known rRNA methylation sites. This was strongly supported by analyses of individual snoRNA interactions e.g. U14, which is known to interact at two positions on the 18S rRNA sequence (Figure 1D). We conclude that both CLASH and FLASH provide consistent and reliable results. However, the background in FLASH analyses appeared higher than with CLASH, presumably reflecting the lower stringency of purification.

Identification of novel snoRNA-rRNA interaction sites

Modification sites in ribosomal RNAs have been well characterized by a variety of highly sensitive techniques, and it is very likely that all high-efficiency methylation sites have been identified (see (Marchand et al., 2016; Taoka et al., 2016) and references therein). Nonetheless, sub-stoichiometric modifications may have escaped direct identification. If these are mediated by

a box C/D snoRNA, a hybrid must form that may be captured by CLASH. We therefore developed robust bioinformatics filters for snoRNA-rRNA interactions, to confidently identify putative novel sites of methylation.

We use the following strict filtering criteria to identify interactions that we can classify with high confidence as being capable of guiding methylation (Figure 2):

- Nucleotide 5 bps upstream of D box or D' box in snoRNA base pairs exactly with rRNA and hybrid contains 12 or more base-paired nucleotides
- One or more nucleotides in region between 2 and 4 bps upstream of D box or D' box base pairs exactly with rRNA
- There is not exact base pairing over the whole D or D' box
- Either:
  - There is a stretch of eight nucleotides between 1 and 14 bps upstream of D box or D' box base pair exactly with rRNA (no mismatches), or
  - There is a stretch of eleven nucleotides between 1 and 16 bps upstream of D box or D' box base pair exactly with rRNA with at most 1 mismatch

For each of the above criteria, G-U base pairs are not counted as exact base pairing.

We recovered 9,363 hybrids passing these criteria and thus potentially able to guide methylation In addition to known methylation sites we recovered novel snoRNA-rRNA interactions that could potentially guide methylation, including an orphan snoRNA SNORD126 (Figure 3; Supplementary Table S2). For SNORD14 (U14) interactions were recovered that would potentially guide methylation at 18S-462 and 18S-83. We conclude that the filters are quite conservative, and should recover only interactions with a high likelihood of representing methylation-guide RNA binding sites.

Due to the strict criteria, many confirmed methylation site interactions were filtered out. In order to ensure that hybrids that did not meet these strict criteria but were associated with methylation site interactions were not included in downstream analyses, we also used a weaker set of criteria to identify potentially methylating hybrids. Hybrids were classified as potentially methylating hybrids if they did not meet the strict methylation criteria, but the nucleotide 5 base pairs upstream of the D or D' box did base pair with the rRNA. Unlike the strict criteria, these weaker criteria did allow G-U base pairs. We recovered 7,971 hybrids passing these criteria,

11

representing 412 interactions, including additional known methylation guide interactions for which no hybrids were found that passed the strict methylation criteria (Table S3).

The hybrids that did not meet the strict or lenient methylation criteria, and whose pre-47S fragment did not overlap with a nucleotide for which the snoRNA included in the hybrid was known to guide methylation, were separated in three further categories: 'ancillary' (Table S4), 'blocking' (Table S5), or 'structural' hybrids (Table S6), depending on whether they potentially assist or interfere with the methylation function of a snoRNA, or contribute to pre-rRNA folding during ribosomal subunit assembly (Figure 2).

Hybrids recovered 100 nt upstream or downstream of a methylation site directed by the same snoRNA, but not overlapping with it, were designated "ancillary" as they could give additional structural support to the guide snoRNA interaction (Figure S3A; Supplementary Table S1) (van Nues et al., 2011). We recovered 692 ancillary hybrids.

Hybrids formed by snoRNAs at methylation site, that are not predicted to guide methylation but forming at least 22 perfect Watson-Crick pairs within 17 nt upstream or downstream of the site were called "blocking" interactions. In total, 11,028 non-methylating hybrids overlapped with interactions guiding methylation (Supplementary Table S1). Among these interactions, the majority guide methylation at neighboring sites. It is unlikely that closely located sites (less than 20 nt separation) could be methylated. Thus, over-expression of a snoRNA could lead to both increased methylation at its target rRNA site and suppression at neighboring sites. The presence of such overlapping methylation guide interaction sites suggests the need for a precise timing for snoRNA binding and methylation; such an ordered sequence may contribute to the correct folding of the pre-rRNAs and/or aid in avoiding kinetic traps (Huang and Karbstein, 2021; Steitz and Tycowski, 1995). For clarity, these interactions were not included in the "blocking" interactions list. However, 62 high confidence blocking hybrids were identified for snoRNAs that are not predicted to direct methylation at closely located sites (Figure S3B; Supplementary Table S1). Recent reports have highlighted the variability in methylation efficiency at different sites in the human rRNA (Erales et al., 2017; Krogh et al., 2016; Sharma et al., 2017a; Zhou et al., 2017):, and we speculate that this may partly reflect competition for binding between snoRNA species. For instance, we observed interactions involving the abundant snoRNAs U3 and U8 that could block methylation sites.

All other confidently identified snoRNA-rRNA hybrids were termed "structural" interactions, reflecting potential structural roles in supporting conformational changes and avoiding kinetic traps during pre-ribosome assembly and/or pre-rRNA folding (Huang and Karbstein, 2021; Steitz and Tycowski, 1995). These included the small number of box C/D snoRNAs implicated in ribosome synthesis steps other than rRNA methylation (Figure S3C): U3, U8, U14 and the acetylation guide U13.

Among novel structural interactions, we found hybrids between 18S rRNA and the 3' region of U8 snoRNA. It was previously reported that the 5' end of U8 snoRNA is critical for 5.8S and 28S rRNA maturation (Peculis, 1997). However, no interactions for the 3' region of U8 were described and the functional significance remains to be established. In *Xenopus*, the timing of association of the 3' end of 5.8S rRNA and 5' end of 28S was proposed to be regulated by initial binding of U8 at the 5' end of 28S, promote formation of a "bulge" in the 28S sequence. This might act as a "priming site" for base-pairing to 5.8S, leading to the eventual displacement of U8. We note that a peak of U8 interaction is located at the 5' end of 28S (Figure 4B), potentially corresponding to this predicted interaction.

Novel snoRNA-snoRNA interactions

Many reproducible snoRNA-snoRNA hybrids were recovered (261,166) (Supplementary Table S1), but these predominately represented internal stems, particularly within U3 (229,525 hybrids). However, we also recovered 14,235 reproducible intermolecular hybrids between different snoRNA species, representing 1,422 distinct interactions (Figures S4A and S4B). These interactions suggest the existence of regulatory loops in snoRNA biogenesis and function, e.g. through possible titration/sequestration or "sponging". In addition, a small number of interactions predicted to guide snoRNA methylation were detected (Figure S4C), using the same criteria as applied to rRNA (Figure 2).

snoRNA-tRNA interactions

We noted that although tRNAs represented only a small proportion of all snoRNA hybrids (0.2%), they were enriched for interactions that potentially direct methylation. Overall, from 591 reproducible snoRNA-tRNA hybrids, two met the criteria for classification as high confidence methylating hybrids, and 161 met the criteria for classification as potentially methylating hybrids. Notably, for hybrids between snoRNAs and tRNAs that contain introns, 63% (71 out of 113 reproducible hybrids) were classified as high confidence or potentially directing methylation. In

13

contrast, for hybrids between snoRNAs and tRNAs that do not contain introns, only 19% (92 of 478 reproducible hybrids) meet these criteria (Supplementary Table 1).

snoRNA-mRNA interactions

Perhaps the most interesting class of snoRNA chimeras involved snoRNA-mRNA interactions. It has been proposed that snoRNAs can influence pre-mRNA splicing, processing and stability in mammalian cells; for examples see (Falaleeva et al., 2015; Huang et al., 2017; Kishore and Stamm, 2006; Sharma et al., 2016). It is, however, also possible that snoRNAs might be sponged on abundant mRNAs.

Among reproducible, stable hybrids, 28,120 snoRNA-mRNA hybrids were recovered, representing 1,755 interactions between 149 snoRNA families and 967 mRNAs. To eliminate potential mis-mapping errors we removed all hybrids that were called as snoRNA-mRNA hybrids, but whose mRNA fragment could also be aligned to U3 or to an rRNA sequence (albeit poorly). This filtering step retained 7,209 hybrids involving 117 snoRNAs and 940 mRNAs.

The greatest number of filtered mRNA interactions was observed for U3 (50% of reproducible snoRNA-mRNA hybrids, interacting with 566 different mRNAs), followed by SNORD33 (8% of hybrids, 23 mRNAs), SNORD24 (3% of hybrids, 15 mRNAs), snoU83B (3% of hybrids, 63 mRNAs), and SNORD58 (3% of hybrids, 37 mRNAs). There was a clear correlation for mRNAs between filtered hybrids and single hits (p = $6e^{-166}$), showing enrichment of mRNA single hits in the regions of snoRNA interactions (Figure 5B). In contrast, there was little correlation between mRNA expression levels and recovery in snoRNA hybrids (R^2=0.0057) (Figure 5C). These data support the conclusion that target mRNAs were specifically recovered and represent *bona fide* interactions.

To assess whether novel snoRNA-mRNA interactions have the potential to direct RNA methylation, the hybrids were analyzed using the same criteria those applied to rRNA (Figure 2). This identified a small number of putative methylation guide interactions (Supplementary Figure S7).

Comparison of snoRNA-mRNA interactions revealed distinctly different patterns of targets between U3 and other snoRNAs (Figure 6A). Interactions with all snoRNAs were recovered in mRNA coding sequences (CDS) and untranslated regions (UTRs), but were substantially

14

enriched in pre-mRNA introns (Figure 6A). However, more CDS interactions were recovered for U3 than for all other snoRNAs combined. Those U3 interactions that were identified within mRNA introns were predominately not in proximity to splice junctions. Moreover, most mRNA-U3 binding sites presented sharp peaks pointing to highly-specific interactions. The strikingly high number of U3-mRNA interactions suggest a special role for U3 in mammalian gene expression, which might be reflected in the substantially greater abundance of U3 than other human snoRNAs and detection of stable abundant U3-derived fragments.

To study the functional role of U3 interactions we depleted U3 in HEK cells with morpholino oligo and carried out transcriptome analyses of control (mock treated) and U3-depleted cells. RNA sequencing showed that 3 days following U3 depletion, substantially more mRNAs identified as U3 targets in CLASH showed altered levels than non-targets or total genes (Chi Square Test; p = $4e^{-6}$). U3 target RNAs showed both increased and decreased levels, but 20% of CLASH/FLASH U3 targets showed reduced abundance after U3 depletion (Supplementary Figure S8B). Notably, we observed a correlation between the presence of a snoRNA targeted by U3 in the intron and levels of its host mRNA after U3 depletion, pointing to general rule of interplay between biogenesis of snoRNAs and their host genes.

Initial comparison of the binding sites to the patterns of evolutionary conservation across 23 mammalian species did not identify enrichment for conserved regions in snoRNA binding sites relative to their flanking regions. However, further analysis revealed that the fall in conservation was due to the frequent presence of an exon near the snoRNA binding site. The 3' region of introns that bind snoRNAs was more conserved than, for instance, the 5' region of the same intron not harboring interactions. This observation supports the functional importance of the interactions (Supplementary Figure S6).

Binding is frequently found within introns that host snoRNAs

We noted that a substantial proportion of snoRNA hybrids with intronic regions represented interactions between snoRNAs and their host introns (5% or 220 hybrids), suggesting frequent connections between snoRNA biogenesis and host gene splicing (Figure 6). Around 16% of all C/D snoRNA-mRNA interactions were represented by peaks towards the 3' ends of introns, *in cis* or *in trans,* in the region of potential intron branch point (25 to 50 bp from the 3' SS) (Figure 6) pointing to the possibility of their involvement in splicing of the target mRNAs.

15

Intronic snoRNAs frequently formed predicted duplexes with the 3' flanking region that included the intron branch point and/or of the polypyrimidine tract, both of which are important signals for pre-mRNA splicing. For examples see Figure 7. We speculate that these interactions may slow pre-mRNA splicing allowing sufficient time for assembly of snoRNP proteins with the nascent transcript prior to pre-mRNA intron cleavage and degradation.

DISCUSSION

Here we systematically mapped the interactions between box C/D snoRNAs and the human transcriptome by the use of UV crosslinking, followed by generation and sequencing of RNA hybrids. To achieve high specificity and robustness, we used two complementary approaches: CLASH relies on high-affinity purification tags, suitable for extensive washes in denaturing conditions, whereas FLASH utilizes specific antibodies in combination with mild chemical crosslinking with formaldehyde to stabilize the interactions. Comparison of snoRNA hybrids recovered with CLASH and FLASH revealed a high degree of overlap, and we therefore combined these datasets for most analyses.

As expected, we recovered many interactions between the cognate snoRNAs and known or predicted sites of rRNA methylation. It was, however, notable that at many sites of methylation the human rRNA, multiple snoRNAs could be identified with complementary base-pairing that matched the features previously defined as required for 2'-*O*-methylation; ≥12 bp showing perfect complementarity, with the modified nucleotide positioned 5 bp from a site D motif (Kiss-László et al., 1996). In several cases previously predicted snoRNAs were not recovered, although these may well bind under altered metabolic conditions, in different cells types or during cell differentiation and tumorigenesis. These data underline the surprisingly high degree of plasticity and redundancy in human snoRNA-rRNA interactions. Recent quantitative analyses of human rRNA methylation have identified many sites that show partial methylation suggesting that functionally distinct ribosomes are generated under different growth conditions (Erales et al., 2017; Hebras et al., 2020; Krogh et al., 2016; Sharma et al., 2017a). We also found numerous cases in which snoRNAs were recovered bound to the pre-rRNA close to methylation sites with strong Watson-Crick base-pairing, but in a configuration that is not expected to guide RNA modification. We speculate that these interactions regulate the timing and/or efficiency of rRNA modification by competing with cognate methylation-guide snoRNAs. In addition, they may contribute to pre-rRNA folding dynamics during ribosomal subunit biogenesis, as previously

16

proposed (Huang and Karbstein, 2021; Steitz and Tycowski, 1995). The emergence of snoRNAs with overlapping specificities and overlapping binding sites, indicate that the site-specific regulation of rRNA methylation is both functionally important and complex.

A large number of reproducible snoRNA-mRNA hybrids represented snoRNA-mRNA interactions. Human U3 is 20-50 fold more abundant than most methylation-guide snoRNAs and was responsible for 50% of all filtered snoRNA-mRNA hybrids. These interactions involved a 3' sequence in U3, homologous to a guide region in yeast U3 previously implicated in non-canonical interactions (Dudnakova et al., 2018; Kudla et al., 2011). Following U3 depletion, mRNAs identified as bound by U3 were highly over-represented among mRNAs showing altered abundance. Moreover, U3 target sites were largely located in exons, whereas other snoRNAs predominately target conserved regions of pre-mRNA introns. However, the mechanistic links between U3 interactions and altered mRNA abundance remain unclear. Notably, snoRNA-mRNA interactions did not resemble those formed by miRNAs in structure, distribution or, most likely, in function. The length distribution of the snoRNA fragment of snoRNA-mRNA chimeras showed an average length of around 35 to 40-nt with base pairing region of at least 12nt. This is much longer than expected for miRNA interactions. We also did not observe accumulation of the previously reported, short (≤ 22nt), miRNA-like fragments of snoRNAs in single reads.

In human cells, the majority of snoRNA genes are located within introns in protein coding genes. It was previously suggested that processing of snoRNAs and splicing of the host gene may be connected (Hirose et al., 2003). Indeed, folding of the snoRNA snoRD86, which is encoded in an intron of the NOP56 gene, acts as sensor in controlling the abundance of this snoRNP core protein (Lykke-Andersen et al., 2018). We observed that intronic regions flanking snoRNAs were frequently recovered in hybrids with the same snoRNA, as well as with other snoRNAs. We suggest that such interactions facilitate coordination between the maturation of snoRNA and splicing of the host gene. Debranched introns are expected to be rapidly degraded by both the 5' exonuclease Xrn2 and 3' exonucleases of the exosome complex. It is therefore important that snoRNA folding and snoRNP assembly precedes intron excision. The observed interactions may coordinate these steps.

Despite the essential roles they play during ribosome biogenesis through their involvement in pre-rRNA modification, processing, and folding remains unclear to what extent box C/D snoRNAs contribute to regulating the homeostasis of other cellular RNAs, including mRNAs. The

17

data on interaction sites reported here may aid the elucidation of non-conventional roles of box C/D snoRNAs and the potential links between altered expression and cell differentiation, embryogenesis or human disease.

DATA ACCESS

All sequence data from this study have been submitted to the NCBI Gene Expression Omnibus (GEO).

www.ncbi.nlm.nih.gov/geo/query/acc.cgi?acc=GSE114825

www.ncbi.nlm.nih.gov/geo/query/acc.cgi?acc=GSE121414

www.ncbi.nlm.nih.gov/geo/query/acc.cgi?acc=GSE121415

DISCLOSURE DECLARATION

The authors declare that they have no competing interests.

REFERENCES

Badrock, A.P., Uggenti, C., Wacheul, L., Crilly, S., Jenkinson, E.M., Rice, G.I., Kasher, P.R., Lafontaine, D.L.J., Crow, Y.J., and O'Keefe, R.T. (2020). Analysis of U8 snoRNA Variants in Zebrafish Reveals How Bi-allelic Variants Cause Leukoencephalopathy with Calcifications and Cysts. Am J Hum Genet *106*, 694-706.

Bergeron, D., Laforest, C., Carpentier, S., Calvé, A., Fafard-Couture, É., Deschamps-Francoeur, G., and Scott, M.S. (2021). SnoRNA copy regulation affects family size, genomic location and family abundance levels. BMC Genomics *22*, 414.

Bharathavikru, R., Dudnakova, T., Aitken, S., Slight, J., Artibani, M., Hohenstein, P., Tollervey, D., and Hastie, N. (2017). Transcription factor Wilms' tumor 1 regulates developmental RNAs through 3′ UTR interaction. Genes Dev *31*, 347-352.

Bieth, E., Eddiry, S., Gaston, V., Lorenzini, F., Buffet, A., Conte Auriol, F., Molinas, C., Cailley, D., Rooryck, C., Arveiler, B.*, et al.* (2015). Highly restricted deletion of the SNORD116 region is implicated in Prader-Willi Syndrome. Eur J Hum Genet *23*, 252-255.

Bouchard-Bourelle, P., Desjardins-Henri, C., Mathurin-St-Pierre, D., Deschamps-Francoeur, G., Fafard-Couture, É., Garant, J.-M., Elela, S.A., and Scott, M.S. (2019). snoDB: an interactive database of human snoRNA sequences, abundance and interactions. Nucleic Acids Res *48*, D220-D225.

Bouchard-Bourelle, P., Desjardins-Henri, C., Mathurin-St-Pierre, D., Deschamps-Francoeur, G., Fafard-Couture, É., Garant, J.M., Elela, S.A., and Scott, M.S. (2020). snoDB: an interactive database of human snoRNA sequences, abundance and interactions. Nucleic Acids Res *48*, D220-d225.

Bratkovič, T., Božič, J., and Rogelj, B. (2020). Functional diversity of small nucleolar RNAs. Nucleic Acids Res *48*, 1627-1651.

Burnett, L.C., Hubner, G., LeDuc, C.A., Morabito, M.V., Carli, J.F.M., and Leibel, R.L. (2017). Loss of the imprinted, non-coding Snord116 gene cluster in the interval deleted in the Prader Willi syndrome results in murine neuronal and endocrine pancreatic developmental phenotypes. Human Molecular Genetics, ddx342-ddx342.

Cavaillé, J. (2017). Box C/D small nucleolar RNA genes and the Prader-Willi syndrome: a complex interplay. WIREs RNA *8*, e1417.

Dudnakova, T., Dunn-Davies, H., Peters, R., and Tollervey, D. (2018). Mapping targets for small nucleolar RNAs in yeast. Wellcome Open Res *3*, 120.

Dupuis-Sandoval, F., Poirier, M., and Scott, M.S. (2015). The emerging landscape of small nucleolar RNAs in cell biology. WIREs RNA *6*, 381-397.

Erales, J., Marchand, V., Panthu, B., Gillot, S., Belin, S., Ghayad, S.E., Garcia, M., Laforêts, F., Marcel, V., Baudin-Baillieu, A.*, et al.* (2017). Evidence for rRNA 2′-O-methylation plasticity: Control of intrinsic translational capabilities of human ribosomes. Proc Natl Acad Sci USA *114*, 12934-12939.

Fafard-Couture, É., Bergeron, D., Couture, S., Abou-Elela, S., and Scott, M.S. (2021). Annotation of snoRNA abundance across human tissues reveals complex snoRNA-host gene relationships. Genome biology *22*, 172.

Falaleeva, M., Pages, A., Matuszek, Z., Hidmi, S., Agranat-Tamir, L., Korotkov, K., Nevo, Y., Eyras, E., Sperling, R., and Stamm, S. (2016). Dual function of C/D box small nucleolar RNAs in rRNA modification and alternative pre-mRNA splicing. Proc Natl Acad Sci USA *113*, E1625-E1634.

Falaleeva, M., Surface, J., Shen, M., de la Grange, P., and Stamm, S. (2015). SNORD116 and SNORD115 change expression of multiple genes and modify each other's activity. Gene.

Frenk, S., Oxley, D., and Houseley, J. (2014). The Nuclear Exosome Is Active and Important during Budding Yeast Meiosis. PLoS ONE *9*, e107648.

Hebras, J., Krogh, N., Marty, V., Nielsen, H., and Cavaillé, J. (2020). Developmental changes of rRNA ribose methylations in the mouse. RNA Biol *17*, 150-164.

Helwak, A., Kudla, G., Dudnakova, T., and Tollervey, D. (2013). Mapping the human miRNA interactome by CLASH reveals frequent non-canonical binding. Cell *153*, 654-665.

Helwak, A., and Tollervey, D. (2014). Mapping the miRNA interactome by cross-linking ligation and sequencing of hybrids (CLASH). Nat Protocols *9*, 711-728.

Henras, A.K., Plisson-Chastang, C., Humbert, O., Romeo, Y., and Henry, Y. (2017). Synthesis, Function, and Heterogeneity of snoRNA-Guided Posttranscriptional Nucleoside Modifications in Eukaryotic Ribosomal RNAs. Enzymes *41*, 169-213.

Hirose, T., Shu, M.D., and Steitz, J.A. (2003). Splicing-dependent and -independent modes of assembly for intron-encoded box C/D snoRNPs in mammalian cells. Mol Cell *12*, 113-123.

Huang, C., Shi, J., Guo, Y., Huang, W., Huang, S., Ming, S., Wu, X., Zhang, R., Ding, J., Zhao, W.*, et al.* (2017). A snoRNA modulates mRNA 3′ end processing and regulates the expression of a subset of mRNAs. Nucleic Acids Research *45*, 8647-8660.

Huang, H., and Karbstein, K. (2021). Assembly factors chaperone ribosomal RNA folding by isolating helical junctions that are prone to misfolding. Proceedings of the National Academy of Sciences of the United States of America *118*.

Jorjani, H., Kehr, S., Jedlinski, D.J., Gumienny, R., Hertel, J., Stadler, P.F., Zavolan, M., and Gruber, A.R. (2016). An updated human snoRNAome. Nucleic Acids Res *44*, 5068-5082.

Kishore, S., and Stamm, S. (2006). The snoRNA HBII-52 Regulates Alternative Splicing of the Serotonin Receptor 2C. Science *311*, 230-232.

Kiss-László, Z., Henry, Y., Bachellerie, J.-P., Caizergues-Ferrer, M., and Kiss, T. (1996). Site-specific ribose methylation of preribosomal RNA: A novel function for small nucleolar RNAs. Cell *85*, 1077-1088.

Knox, A.A., McKeegan, K.S., Debieux, C.M., Traynor, A., Richardson, H., and Watkins, N.J. (2011). A weak C' box renders U3 snoRNA levels dependent on hU3-55K binding. Molecular and cellular biology *31*, 2404-2412.

Krogh, N., Jansson, M.D., Häfner, S.J., Tehler, D., Birkedal, U., Christensen-Dalsgaard, M., Lund, A.H., and Nielsen, H. (2016). Profiling of 2′-O-Me in human rRNA reveals a subset of

fractionally modified positions and provides evidence for ribosome heterogeneity. Nucleic Acids Res *44*, 7884-7895.

Kudla, G., Granneman, S., Hahn, D., Beggs, J., and Tollervey, D. (2011). Mapping in vivo RNA-RNA interactions by crosslinking, ligation and sequencing of hybrids. Proc Natl Acad Sci USA *108*, 10010-10015.

Langhendries, J.-L., Nicolas, E., Doumont, G., Goldman, S., and Lafontaine, D.L.J. (2016). The human box C/D snoRNAs U3 and U8 are required for pre-rRNA processing and tumorigenesis. Oncotarget; Vol 7, No 37.

Lorenz, R., Bernhart, S.H., Höner zu Siederdissen, C., Tafer, H., Flamm, C., Stadler, P.F., and Hofacker, I.L. (2011). ViennaRNA Package 2.0. Algorithms for Molecular Biology *6*, 26.

Lowe, T.M., and Eddy, S.R. (1999). A computational screen for methylation guide snoRNAs in yeast. Science *283*, 1168-1171.

Lu, Z., Zhang, Qiangfeng C., Lee, B., Flynn, Ryan A., Smith, Martin A., Robinson, James T., Davidovich, C., Gooding, Anne R., Goodrich, Karen J., Mattick, John S.*, et al.* (2016). RNA Duplex Map in Living Cells Reveals Higher-Order Transcriptome Structure. Cell *165*, 1267-1279.

Lykke-Andersen, S., Ardal, B.K., Hollensen, A.K., Damgaard, C.K., and Jensen, T.H. (2018). Box C/D snoRNP Autoregulation by a cis-Acting snoRNA in the NOP56 Pre-mRNA. Mol. Cell *72*, 99-111.e115.

Marchand, V., Blanloeil-Oillo, F., Helm, M., and Motorin, Y. (2016). Illumina-based RiboMethSeq approach for mapping of 2′-O-Me residues in RNA. Nucleic Acids Research *44*, e135-e135.

Omer, A.D., Lowe, T.M., Russell, A.G., Ebhardt, H., Eddy, S.R., and Dennis, P.P. (2000). Homologs of small nucleolar RNAs in Archaea. Science *288*, 517-522.

Peculis, B.A. (1997). The sequence of the 5' end of the U8 small nucleolar RNA is critical for 5.8S and 28S rRNA maturation. Mol Cell Biol *17*, 3702-3713.

Rozhdestvensky, T.S., Robeck, T., Galiveti, C.R., Raabe, C.A., Seeger, B., Wolters, A., Gubar, L.V., Brosius, J., and Skryabin, B.V. (2016). Maternal transcription of non-protein coding RNAs from the PWS-critical region rescues growth retardation in mice. Scientific Reports *6*, 20398.

Sharma, E., Sterne-Weiler, T., O'Hanlon, D., and Blencowe, Benjamin J. (2016). Global Mapping of Human RNA-RNA Interactions. Mol Cell *62*, 618-626.

Sharma, S., Langhendries, J.-L., Watzinger, P., Kötter, P., Entian, K.-D., and Lafontaine, D.L.J. (2015). Yeast Kre33 and human NAT10 are conserved 18S rRNA cytosine acetyltransferases that modify tRNAs assisted by the adaptor Tan1/THUMPD1. Nucleic Acids Research *43*, 2242-2258.

Sharma, S., Marchand, V., Motorin, Y., and Lafontaine, D.L.J. (2017a). Identification of sites of 2'-O-methylation vulnerability in human ribosomal RNAs by systematic mapping. Sci Rep *7*, 11490.

Sharma, S., Yang, J., van Nues, R., Watzinger, P., Kötter, P., Lafontaine, D.L.J., Granneman, S., and Entian, K.-D. (2017b). Specialized box C/D snoRNPs act as antisense guides to target RNA base acetylation. PLOS Genetics *13*, e1006804.

Siprashvili, Z., Webster, D.E., Johnston, D., Shenoy, R.M., Ungewickell, A.J., Bhaduri, A., Flockhart, R., Zarnegar, B.J., Che, Y., Meschi, F*., et al.* (2016). The noncoding RNAs SNORD50A and SNORD50B bind K-Ras and are recurrently deleted in human cancer. Nat Genet *48*, 53-58.

Sloan, K.E., Warda, A.S., Sharma, S., Entian, K.-D., Lafontaine, D.L.J., and Bohnsack, M.T. (2017). Tuning the ribosome: The influence of rRNA modification on eukaryotic ribosome biogenesis and function. RNA Biology *14*, 1138-1152.

Steitz, J., and Tycowski, K. (1995). Small RNA chaperones for ribosome biogenesis. Science *270*, 1626-1627.

Su, H., Xu, T., Ganapathy, S., Shadfan, M., Long, M., Huang, T.H.M., Thompson, I., and Yuan, Z.M. (2013). Elevated snoRNA biogenesis is essential in breast cancer. Oncogene, advance online publication 1 April 2013; doi: 2010.1038/onc.2013.2089.

Sugimoto, Y., Vigilante, A., Darbo, E., Zirra, A., Militti, C., D/'Ambrogio, A., Luscombe, N.M., and Ule, J. (2015). hiCLIP reveals the in vivo atlas of mRNA secondary structures recognized by Staufen 1. Nature *519*, 491-494.

Taoka, M., Nobe, Y., Yamaki, Y., Yamauchi, Y., Ishikawa, H., Takahashi, N., Nakayama, H., and Isobe, T. (2016). The complete chemical structure of Saccharomyces cerevisiae rRNA: partial pseudouridylation of U2345 in 25S rRNA by snoRNA snR9. Nucleic Acids Research *44*, 8951-8961.

Thorenoor, N., and Slaby, O. (2015). Small nucleolar RNAs functioning and potential roles in cancer. Tumor Biol *36*, 41-53.

Tollervey, D., and Kiss, T. (1997). Function and synthesis of small nucleolar RNAs. Curr Opin Cell Biol *9*, 337-342.

Travis, A.J., Moody, J., Helwak, A., Tollervey, D., and Kudla, G. (2014). Hyb: A bioinformatics pipeline for the analysis of CLASH (crosslinking, ligation and sequencing of hybrids) data. Methods *65*, 263-273.

van Nues, R.W., Granneman, S., Kudla, G., Sloan, K.E., Chicken, M., Tollervey, D., and Watkins, N.J. (2011). Box C/D snoRNP catalysed methylation is aided by additional pre-rRNA base-pairing. EMBO J *30*, 2420-2430.

Watkins, N.J., and Bohnsack, M.T. (2012). The box C/D and H/ACA snoRNPs: key players in the modification, processing and the dynamic folding of ribosomal RNA. WIRES: RNA *3*, 397-414.

Xu, G., Yang, F., Ding, C.-L., Zhao, L.-J., Ren, H., Zhao, P., Wang, W., and Qi, Z.-T. (2014). Small nucleolar RNA 113-1 suppresses tumorigenesis in hepatocellular carcinoma. Molecular Cancer *13*, 216.

Youssef, O.A., Safran, S.A., Nakamura, T., Nix, D.A., Hotamisligil, G.S., and Bass, B.L. (2015). Potential role for snoRNAs in PKR activation during metabolic stress. Proc Natl Acad Sci USA *112*, 5023-5028.

Zhou, F., Liu, Y., Rohde, C., Pauli, C., Gerloff, D., Kohn, M., Misiak, D., Baumer, N., Cui, C., Gollner, S.*, et al.* (2017). AML1-ETO requires enhanced C/D box snoRNA/RNP formation to induce self-renewal and leukaemia. Nat Cell Biol *19*, 844-855.

FIGURE LEGENDS

Figure 1. Overview of CLASH and FLASH results

(A) Schematic representation of CLASH and FLASH techniques. Live cells were UV-irradiated, crosslinked RNA–protein complexes were extracted and affinity purified. RNAs were partially digested and interacting RNAs were ligated together to generate hybrid molecules. Following cDNA generation and sequencing, cognate RNA pairs were identified in chimeric cDNAs. In CLASH, complexes were tandem-affinity purified under denaturing conditions. In FLASH, complexes were immuno-purified using antibodies and then crosslinked to the beads, allowing subsequent wash steps under denaturing conditions. (B) Human reproducible hybrid counts by experiment type. Reproducibility of hybrids across CLASH and FLASH experiments in HEK293 cells. (C) All hybrids over 47S pre-rRNA in aggregated CLASH and FLASH experiments. The distributions of snoRNA hybrid hits in CLASH (red) and FLASH (blue) over 47S pre-rRNA show similar peaks, with known methylation sites shown in grey. (D) U14 hybrids over 47S pre-rRNA in aggregated CLASH and FLASH experiments. U14 (SNORD14) hybrids with rRNA in CLASH (red) and FLASH (blue) identify known interaction sites.

Figure 2. Decision rules used to categorize snoRNA-47S pre-rRNA hybrids. The flowchart summarizes the decision rules.

The filtering criteria were applied to reproducible snoRNA-rRNA hybrids to identify those that are likely to guide methylation.

Figure 3. Distribution of predicted cognate snoRNA-rRNA interactions at methylation sites

Predicted sites of C/D box snoRNA guided methylation based on the filtered set of reproducible snoRNA-rRNA hybrids. The x axis labels show the snoRNA, the pre47S subunit and co-ordinate at which methylation is predicted to occur, and the snoRNA box 5 base pairs downstream of the methylating nucleotide. The bars show the number of hybrids associated with the methylation event described in the access label, with the number of experiments in which relevant hybrids were found shown in brackets. Blue bars indicate previously reported methylation sites, and red bars indicate interactions that have not previously been reported to be associated with methylation.

Figure 4. Distribution of selected snoRNAs on the 47S pre-rRNA

(A-C) The distribution of hybrid hits involving U3, U8, and U13, respectively, over the 47S pre-rRNA sequence. Reported methylation sites are shown in grey.

Figure 5. Single hits around snoRNA-mRNA hybrid starts, and correlation of snoRNA-mRNA hybrids with mRNA single hits and abundance

(A) Distribution of single hits around snoRNA-mRNA hybrid starts.

(B) Correlation between recovery in reproducible CLASH hybrids and mRNA single hits.

(C) Correlation between recovery in reproducible CLASH hybrids and mRNA abundance.

Figure 6. Distribution of snoRNA interactions on mRNAs

(A) Counts of hybrids overlapping different mRNA features for snoRNA−mRNA hybrids incorporating U3, and hybrids incorporating other snoRNAs, respectively. The plots show that while both classes of hybrid predominantly bind mRNA introns, hybrids incorporating U3 are significantly more likely to bind other regions of their target RNA. (B) Total overlapping hybrids vs intron / exon ratios for individual snoRNAs in cis and trans. (C-H) CLASH / FLASH hits over the last 1000 base pairs of mRNA introns, with the estimated branch point region (20-50bps upstream of the 3' end of the intron) highlighted in green. Non-U3 hybrids show a pronounced

24

peak overlapping the estimated branch point region in host introns, non-host introns within the host gene, and introns within non-host genes.

Figure 7. Interactions between selected snoRNAs and host introns

(A) Distribution of CLASH single hits across the host intron of SNORD2 in EIF4A2, showing that reads that do not overlap the snoRNA overlap the 3' end of its host intron (B,C) Circos plots showing hybrids between SNORD2, SNORD35A, and SNORD38A, and their host introns. In each case, hybrids are exclusively formed between the snoRNA and the 3' end of its host intron.

A

Schematic representation of CLASH and FLASH techniques
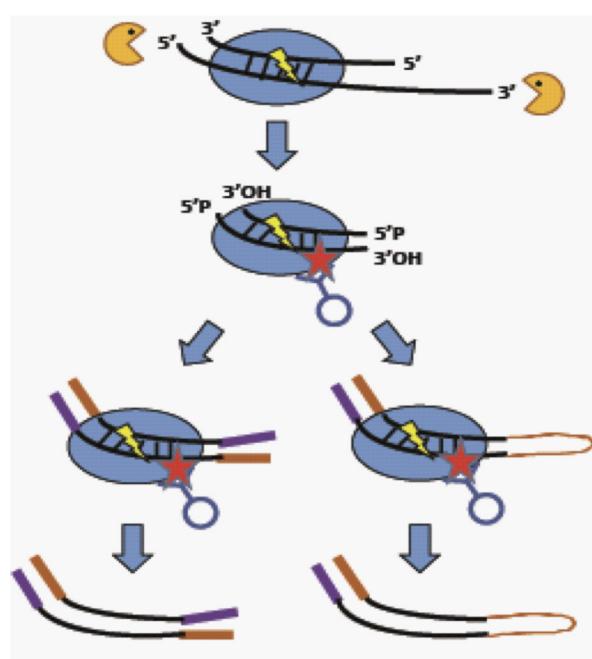
B

Human reproducible hybrid counts by experiment type

C

All hybrids over 47S pre-rRNA in aggregated CLASH and FLASH experiments

D

U14 hybrids over 47S pre-rRNA in aggregated CLASH and FLASH experiments

Dunn-Davies et al. Fig. 1

Decision rules used to categorize snoRNA-47S pre-rRNA hybrids

Reproducible snoRNA-47S hybrid

- Nucleotide 5 bps upstream of D/D' box in the snoRNA base pairs exactly with rRNA and hybrid contains 12 or more base paired nucleotides, and
- One or more nucleotides between 2 and 4 bps upstream of D/D' box base pairs exactly with rRNA, and
- There is no exact base pairing over the D/D' box, and either
- There is a stretch of at least eight nucleotides that base pairs exactly, between 1 and 14 bps upstream of the D/D' box, or
- There is a stretch of at least eleven nucleotides that base pairs with at most one mismatch, between 1 and 16 bps upstream of the D/D' box
- For each of the above criteria, G-U base pairs are not counted as exact base pairing

Passes strict methylation criteria — Yes → **Classify as high confidence methylating hybrid**

No

- Nucleotide 5 bps upstream of D/D' box in the snoRNA base pairs with rRNA. Here G-U base pairs are counted as valid base pairing

Passes loose methylation criteria — Yes → **Classify as potentially methylating hybrid**

No

- List of potential methylation sites combines the list of 47S co-ordinates of reported methylation sites from the literature, and the list of 47S co-ordinates that have been found to base pair exactly with the nucleotide 5 bps upstream of the D/D' box in some snoRNA in the above steps

47S fragment overlaps potential methylation site — Yes → **Classify as overlapping hybrid**

No

Hybrid does not overlap a methylating or overlapping hybrid, and the 47S fragment overlaps the region 100bps upstream or downstream of a methylation site taken from the list of potential methylation sites described above

Meets criteria for ancillary interaction? — Yes → **Classify as hybrid representing ancillary interaction**

No

Hybrid has at least 22 Watson-Crick base pairs within 17 bps upstream or downstream of a methylation site taken from the list of potential methylation sites described above, allowing at most 12 mismatches

Meets criteria for blocking interaction? — Yes → **Classify as hybrid representing blocking interaction**

No

Classify as hybrid representing structural interaction

Dunn-Davies et al. Fig. 2

All predicted snoRNA methylation sites based on high confidence methylating interactions

snoRNA site	Value
SNORD91 : 28S-4588 (D' box)	1,994 (16)
SNORD14 : 18S-462 (D box)	670 (12)
snoZ17 : 18S-121 (D' box)	667 (13)
SNORD27 : 18S-27 (D' box)	653 (9)
SNORD38 : 28S-1858 (D' box)	435 (11)
SNORD25 : 18S-1490 (D box)	427 (10)
SNORD45 : 18S-159 (D box)	417 (10)
SNORD110 : 18S-1288 (D' box)	416 (13)
SNORD14 : 18S-83 (D' box)	299 (11)
SNORD70 : 18S-512 (D box)	277 (12)
snoMBII-202 : 18S-428 (D' box)	259 (12)
SNORD61 : 18S-1442 (D box)	257 (9)
SNORD57 : 18S-99 (D box)	218 (9)
SNORD65 : 18S-627 (D' box)	194 (9)
SNORD24 : 28S-2338 (D box)	194 (10)
SNORD11B : 18S-509 (D box)	182 (9)
SNORD36 : 18S-668 (D box)	165 (2)
SNORD21 : 28S-3682 (D' box)	158 (9)
SNORD31 : 28S-4166 (D' box)	154 (9)
SNORD143, SNORD144 : 28S-2402 (D' box)	153 (10)
SNORD96 : 5.8S-75 (D box)	121 (9)
SNORD42 : 18S-116 (D box)	116 (7)
SNORD20 : 18S-1806 (D box)	110 (9)
SNORD43 : 18S-1705 (D' box)	91 (3)
SNORD105, snoU105B : 18S-799 (D box)	86 (9)
SNORD99 : 28S-2774 (D box)	66 (10)
SNORD5 : 28S-2409 (D' box)	58 (9)
SNORD72 : 28S-4590 (D' box)	53 (2)
SNORD81 : 28S-391 (D' box)	42 (9)
SNORD59 : 18S-1031 (D' box)	41 (2)
snoZ40 : 28S-2411 (D' box)	36 (6)
SNORD35 : 18S-47 (D box)	34 (2)
SNORD45 : 18S-172 (D' box)	33 (8)
SNORD95 : 28S-2802 (D box)	31 (7)
SNORD95 : 28S-2811 (D box)	30 (7)
SNORD125 : 18S-1440 (D box)	30 (8)
SNORD51, SNORD33 : 28S-1511 (D' box)	28 (7)
SNORD26 : 28S-389 (D' box)	28 (7)
SNORD24 : 28S-2350 (D box)	28 (2)
SNORD48 : 28S-1868 (D box)	23 (8)
SNORD18 : 28S-1313 (D' box)	21 (4)
SNORND104 : 28S-1327 (D' box)	17 (5)
SNORD34 : 28S-2824 (D' box)	17 (5)
SNORD63 : 28S-4541 (D' box)	16 (3)
SNORD56 : 18S-517 (D' box)	16 (3)
SNORD87 : 28S-3723 (D' box)	14 (4)
SNORD36 : 28S-3703 (D' box)	13 (1)
SNORD15 : 28S-4662 (D box)	9 (1)
SNORD37 : 28S-3697 (D' box)	8 (2)
SNORD19B : 18S-683 (D box)	8 (2)
SNORD111 : 28S-3923 (D' box)	8 (3)
snoU83B : 18S-189 (D' box)	6 (1)
SNORD15 : 28S-3764 (D box)	5 (4)
SNORD126 : 28S-1310 (D' box)	5 (2)
snoU54 : 18S-644 (D box)	4 (1)
SNORD98 : 18S-867 (D' box)	2 (1)
SNORD62 : 28S-4999 (D' box)	2 (1)
SNORD52 : 28S-3904 (D' box)	2 (1)
SNORD73 : 28S-879 (D' box)	1 (1)
SNORD63 : 28S-4522 (D' box)	1 (1)
SNORD45 : 18S-174 (D' box)	1 (1)

Number of hybrids passing filters (source file count)

Legend: Not reported / Reported

Dunn-Davies et al. Fig. 3

A
U3-pre47S hybrids over pre47S

B
U8-pre47S hybrids over pre47S

C
U13-pre47S hybrids over pre47S

Dunn-Davies et al. Fig. 4

A Single hits around snoRNA-mRNA hybrid starts

B Total HPM, reproducible hybrid barcodes vs single hits

R^2 = 0.18
p = 6e-166

C Total HPM, reproducible hybrid barcodes vs expression

R^2 = 0.0057
p = 5e-06

Dunn-Davies et al. Fig. 5

A Count of snoRNA-mRNA hybrids overlapping mRNA features

B Total overlapping hybrids vs I/E ratio for individual snoRNAs
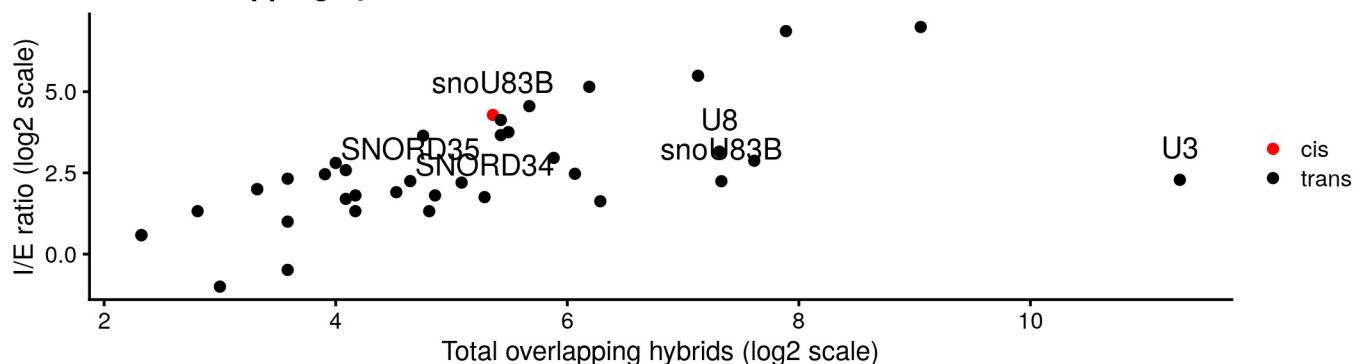
C CLASH/FLASH single hits over last 1000bps of mRNA introns
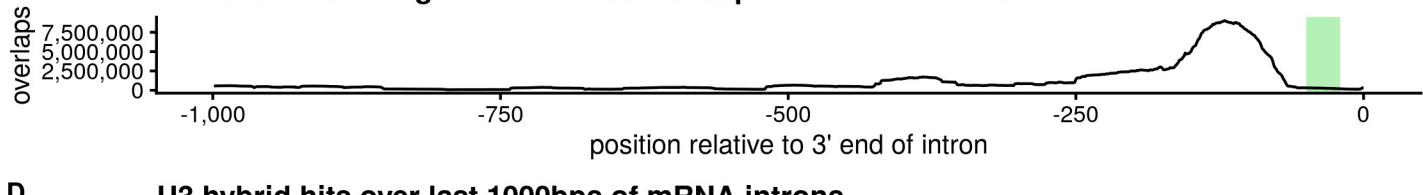
D U3 hybrid hits over last 1000bps of mRNA introns
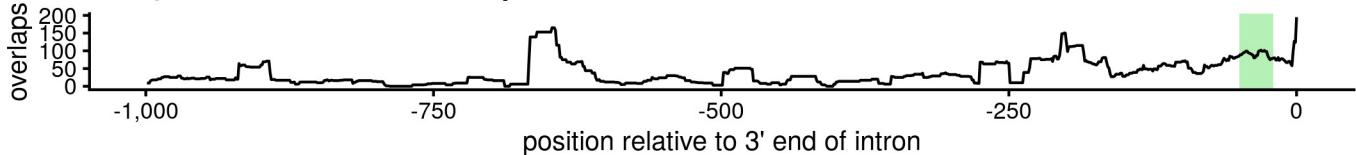
E Non-U3 hybrid hits over last 1000bps of mRNA introns
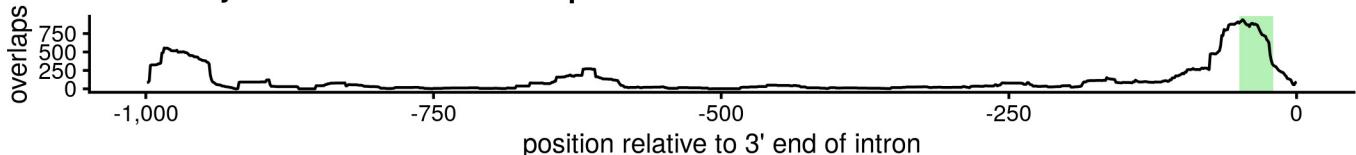
F Non-U3 hybrid hits over last 1000bps of mRNA introns in non-host genes
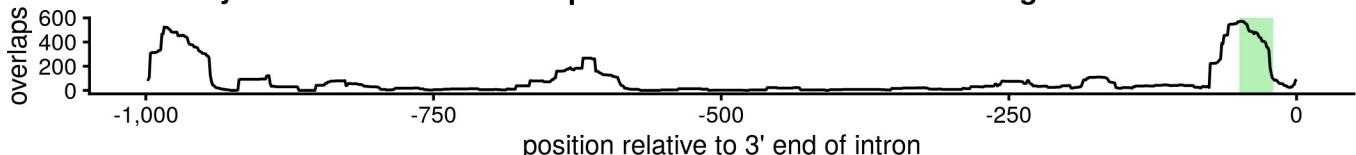
G Non-U3 hybrid hits over last 1000bps of mRNA introns in non-host introns in host genes
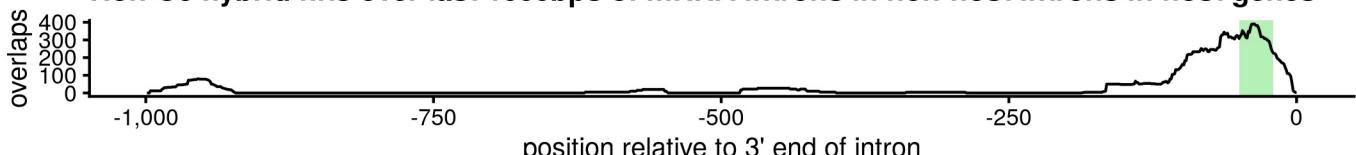
H Non-U3 hybrid hits over last 1000bps of mRNA introns in host introns in host genes

Dunn-Davies et al. Fig. 6

A CLASH single hits across SNORD2 host intron in EIF4A2
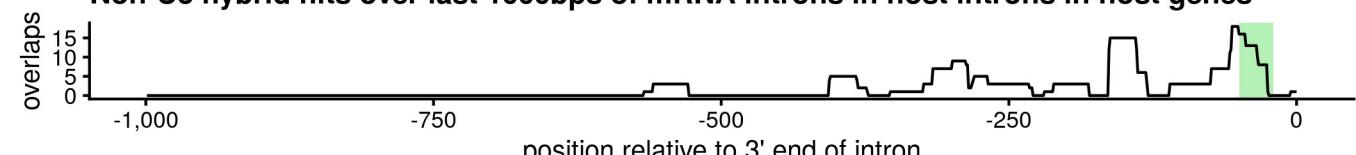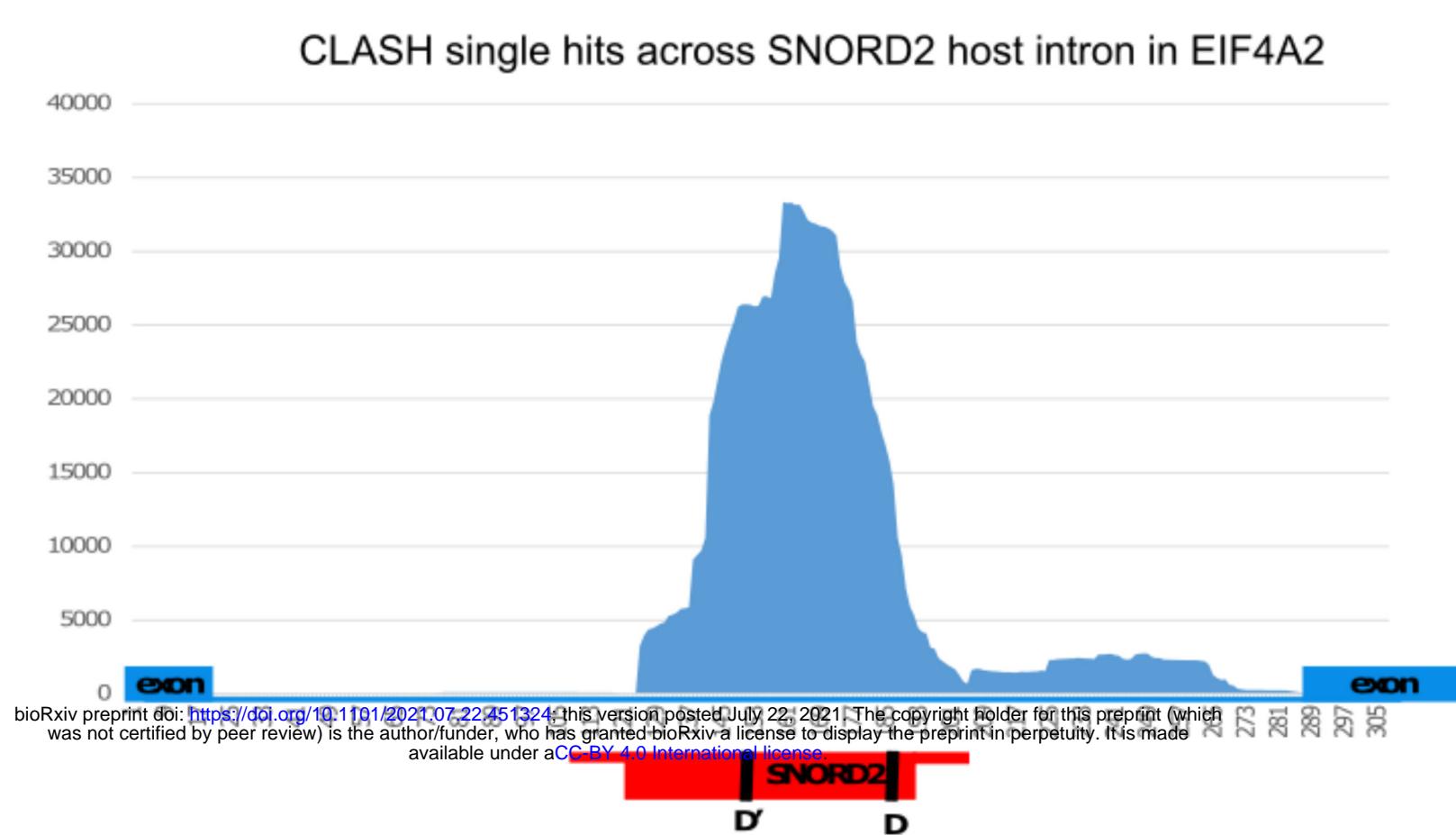
B SNORD2
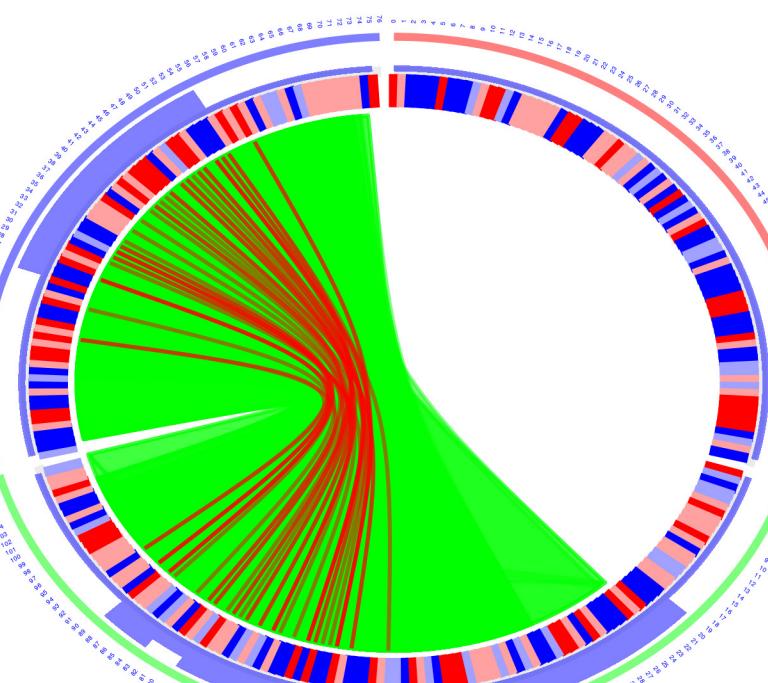
The feature as a line:
- the region before the snoRNA (with flank) is in red
- the snoRNA (with 20bp flanks on each side) is in green
- the region after the snoRNA (and flank) is in blue

Details on the features:
- position of the snoRNA flanks, D and D' boxes
- the estimated branch point on the host mRNA intron

The nucleotide at each position:
A: dark blue
C: light blue
T: light red
G: dark red

C SNORD35A   **D** SNORD38A

Dunn-Davies et al. Fig. 7
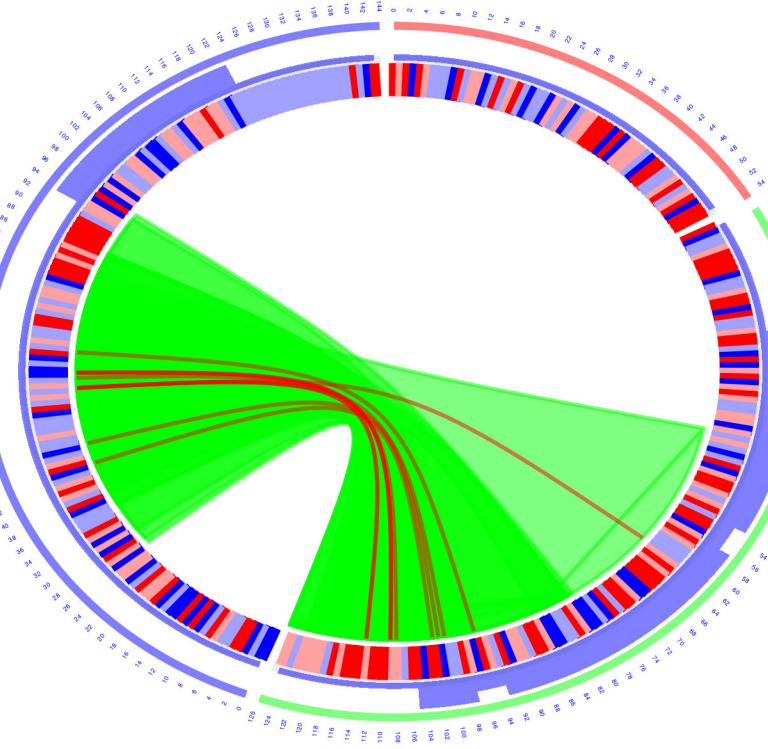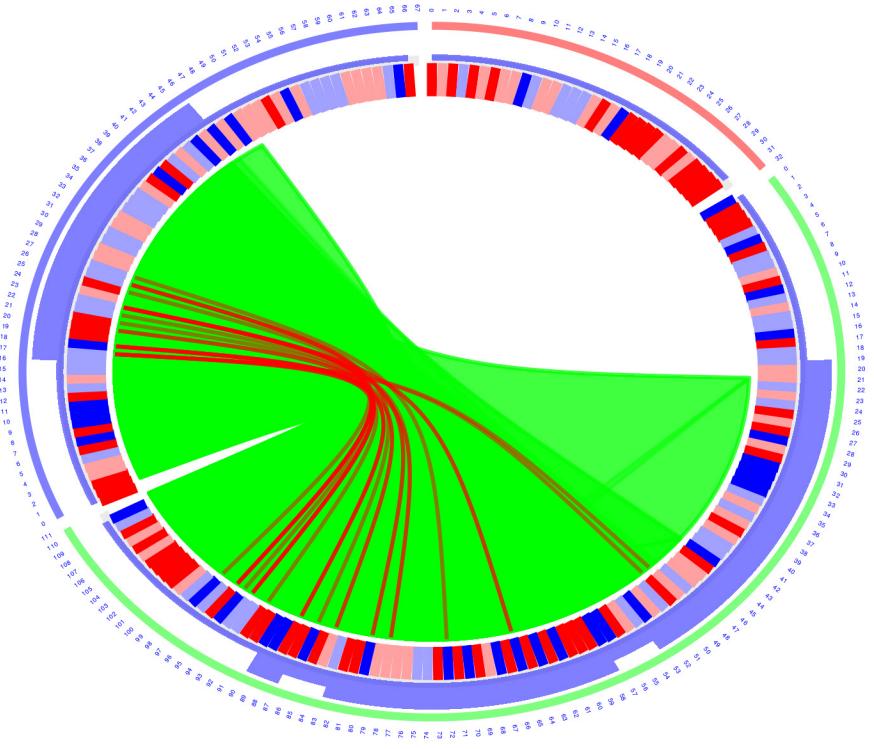
SUPPLEMENTARY MATERIALS

Dataset 1: Interactions recovered

Supplementary Figures

Figure S1. Single hits by biotype

(A) Breakdown of total uncollapsed single hit counts for different RNA biotypes. (B) Breakdown of uncollapsed single hit counts for different RNA biotypes in Fibrillarin CLASH and FLASH experiments. (C) Breakdown of uncollapsed single hit counts for different RNA biotypes in NOP56 CLASH and FLASH experiments. (D) Breakdown of uncollapsed single hit counts for different RNA biotypes in Fibrillarin FLASH experiments.

Figure S2. Hybrids recovered by biotype

(A) Breakdown of hybrid counts in snoRNA hybrids by target RNA biotype. (B) Breakdown of counts of reproducible, stable snoRNA hybrids (with predicted folding energy of -12dG or below) by target RNA biotype.

Figure S3. Classes of non-methylating rRNA interactions

(A, B) Breakdown of snoRNA-pre47S hybrids involved in ancillary interactions and blocking interactions respectively. The x axis labels show the snoRNA families involved, along with the co-ordinate of the relevant methylation site on the pre47S sequence. (C) Breakdown of snoRNA-pre47S hybrids involved in structural interactions. The x axis labels show the relevant snoRNA families.

Figure S4. Characterization of snoRNA-snoRNA interactions

(A) Breakdown of reproducible intermolecular snoRNA-snoRNA hybrids by hybrid type. The hybrid type is obtained by joining the family name of each of the interacting snoRNAs. The order of the snoRNAs is not considered. (B) Breakdown of snoRNA-snoRNA hybrids that pass the filtering criteria described in figure 2A. The x axis labels show the snoRNAs and co-ordinate at which methylation is predicted to occur, and the snoRNA box 5 base pairs downstream of the methylating nucleotide. (C) Counts of snoRNA-snoRNA hybrids predicted to guide methylation with high confidence.

Figure S5. Distribution of length and stability of snoRNA-mRNA hybrids

(A) Histogram of fragment lengths in all hybrids. (B) Histogram of predicted folding energies in all hybrids. (C) Histogram of fragment lengths in reproducible, stable filtered snoRNA-mRNA hybrids with U3 and rRNA filters applied. (D) Histogram of predicted folding energies in reproducible, stable snoRNA-mRNA hybrids with U3 and rRNA filters applied.

Figure S6. Conservation scores of snoRNA-mRNA interactions in human cells

(A) Conservation relative to flanking regions for mRNA fragments of snoRNA-mRNA hybrids involving U3, and non-U3 C/D box snoRNAs, respectively. Beneath each conservation plot is a bar chart showing the distribution of the mRNA fragments of the relevant hybrids between branch point regions of the host gene (host bp), non-branch point regions of the host gene (host non-bp), branch point regions of other genes (other bp) and non-branch point regions of other genes (other non-bp). (B) Conservation relative to flanking regions, split by proportion of hybrids conserved. These plots show that for the majority of interactions and hybrids, there is a clear peak in conservation corresponding to the location of the mRNA fragment of the hybrid. However, there is a small number of interactions with many hybrids that show a large decrease in conservation relative to flanks. This obscures the general pattern of conservation in the overall chart. (C) Three snoRNA-EIF4A2 interactions that show a drop in conservation relative to flanking regions. The three most common interactions with reduced conservation each involves an intron branch point region in EIF4A2. (D) Genome browser track showing the location of the mRNA fragment of SNORD2-EIF4A2 hybrids. In this case, the upstream flanking region overlaps the SNORD2 gene, and the downstream flanking region overlaps an exon of EIF4A2, both of which are highly conserved relative to the intron branch point region bound by the mRNA fragment of the hybrids, explaining the dip in conservation.

Figure S7. Potential methylating interactions with mRNAs

(A) Counts of filtered snoRNA-mRNA hybrids meeting the criteria for classification as high confidence methylating hybrids, broken down by interaction. (B) Counts of filtered snoRNA-mRNA hybrids meeting the criteria for classification as potentially methylating hybrids, broken down by interaction.

Figure S8. Changes in mRNA abundance following U3 depletion

(A) Volcano plot showing the changes in mRNA abundance following 3 days of U3 depletion, compared to a mock control, with U3 targets found in filtered U3-mRNA hybrids highlighted. (B)

Volcano plot showing the changes in mRNA abundance following 2 days of U3 depletion, compared to a mock control, with U3 targets found in filtered U3-mRNA hybrids highlighted.

Figure S9. Filtering steps applied to hybrids

(A) A schematic representation of the filtering steps applied to different classes of RNA-RNA hybrids. Initial, single hit filtering was applied to all hybrids to filter out miscalled single reads. Filtering for reproducibility and stability was then applied to all hybrids. Additional U3 filtering was applied to all hybrids between snoRNAs and other biotypes to filter out miscalled U3-U3 intermolecular hybrids. Finally, additional rRNA filtering was applied to all hybrids between snoRNAs and other non-rRNA biotypes, to filter out miscalled snoRNA-rRNA hybrids. (B) Profile plot showing the distribution of filtered, reproducible SNORD3A (U3) hybrids over SNORD3A by biotype. Each line shows the profile for a different SNORD3A target biotype. The grey shaded regions represent 20 base pair flanking regions upstream and downstream of SNORD3A. The light blue shaded region represents the D box of SNORD3A, the purple line shows the nucleotide 5 base pairs upstream of the D box of SNORD3A, and the light green shaded region represents the D' box of SNORD3A.

A Aggregated single hits (uncollapsed)

snoRNA — 179,038,463 (71.3%)
rRNA — 36,003,746 (14.3%)
mRNA — 24,420,722 (9.7%)
tRNA — 2,985,849 (1.2%)
snRNA — 924,629 (0.4%)
other — 7,616,550 (3.0%)

Number of uncollapsed single hits
(percentage)

B Aggregated Fibrillarin single hits (uncollapsed)

snoRNA — 142,482,682 (74.2%)
rRNA — 24,233,078 (12.6%)
mRNA — 17,412,570 (9.1%)
tRNA — 1,863,111 (1.0%)
snRNA — 718,337 (0.4%)
other — 5,335,171 (2.8%)

Number of uncollapsed single hits
(percentage)

C Aggregated NOP56 single hits (uncollapsed)

snoRNA — 36,555,781 (62.0%)
rRNA — 11,770,668 (20.0%)
mRNA — 7,008,152 (11.9%)
tRNA — 1,122,738 (1.9%)
snRNA — 206,292 (0.3%)
other — 2,281,379 (3.9%)

Number of uncollapsed single hits
(percentage)

D Aggregated Fibrillarin FLASH single hits (uncollapsed)

snoRNA — 19,506,266 (52.3%)
rRNA — 11,479,629 (30.8%)
mRNA — 4,302,193 (11.5%)
snRNA — 136,700 (0.4%)
tRNA — 87,647 (0.2%)
other — 1,760,222 (4.7%)

Number of uncollapsed single hits
(percentage)

Dunn-Davies et al. Fig. S1

A

snoRNA targets in all hybrids by biotype

snoRNA intramolecular — 255,997 (61.0%)
rRNA — 73,374 (17.5%)
mRNA — 52,819 (12.6%)
snoRNA intermolecular — 25,809 (6.1%)
tRNA — 947 (0.2%)
snRNA — 901 (0.2%)
other — 9,866 (2.4%)

Number of hybrids
(percentage)

B

snoRNA targets in reproducible hybrids by biotype

snoRNA intramolecular — 246,931 (70.1%)
rRNA — 57,090 (16.2%)
mRNA — 28,120 (8.0%)
snoRNA intermolecular — 14,235 (4.0%)
tRNA — 591 (0.2%)
snRNA — 306 (0.1%)
other — 4,994 (1.4%)

Number of hybrids
(percentage)

Dunn-Davies et al. Fig. S2

A Ancillary interactions

B Blocking interactions

C Structural interactions

Dunn-Davies et al. Fig. S3

A Counts of reproducible intermolecular snoRNA-snoRNA hybrids involving U3 by type

Type	Count
U3 : snoU83B	1,046 (13.3%)
U8 : U3	828 (10.5%)
U3 : SNORD103	319 (4.0%)
U3 : SNORD23	317 (4.0%)
U3 : SNORD33	266 (3.4%)
U3 : SNORD36	245 (3.1%)
U3 : SNORD12	221 (2.8%)
U3 : SNORD83	186 (2.4%)
U3 : SNORD110	184 (2.3%)
U3 : SNORD58	176 (2.2%)
U3 : SNORD62	165 (2.1%)
U3 : SNORD101	144 (1.8%)
U3 : SNORD2	140 (1.8%)
U3 : SNORD14	133 (1.7%)
others	3,513 (44.6%)

Number of hybrids passing filters (percentage)

B Counts of reproducible intermolecular snoRNA-snoRNA hybrids not involving U3 by type

Type	Count
U8 : SNORD135;ZL2	131 (2.1%)
SNORD36 : SNORD2	115 (1.8%)
SNORD66 : SNORD62	81 (1.3%)
SNORD77 : SNORD58	80 (1.3%)
snoU83B : snoU2_19	79 (1.2%)
U8 : snoU83B	78 (1.2%)
snoU83B : SNORD33	73 (1.1%)
snoU83B : SNORD2	66 (1.0%)
SNORD58 : SNORD2	65 (1.0%)
SNORD62 : SNORD11	58 (0.9%)
U8 : SNORD83	57 (0.9%)
SNORD2 : SNORD103	56 (0.9%)
SNORD58 : SNORD48	54 (0.9%)
U8 : snoU2_19	54 (0.9%)
others	5,305 (83.5%)

Number of hybrids passing filters (percentage)

C Counts of snoRNA-snoRNA hybrids predicted to represent methylation

Type	Count
SNORD19B : SNORD11B-53 (D' box)	7 (1)
SNORD45A : SNORD29-66 (D' box)	6 (1)
SNORD63 : SNORD45A-29 (D' box)	3 (1)
SNORD111B : SNORA26-99 (D' box)	2 (1)
SNORD118 : SNORD117-46 (D box)	2 (1)
SNORD96A : SNORD96A-67 (D box)	2 (2)
SNORD32A : SNORD79-45 (D' box)	1 (1)

Number of hybrids passing filters (experiment count)

Dunn-Davies et al. Fig. S4

A Histogram of fragment lengths in all hybrids

B Histogram of delta G values in all hybrids

C Histogram of fragment lengths in filtered snoRNA-mRNA hybrids

D Histogram of delta G values in filtered snoRNA-mRNA hybrids

Dunn-Davies et al. Fig. S5

A Conservation relative to flanking regions for mRNA fragments of snoRNA-mRNA hybrids by snoRNA type

H/ACA box snoRNA hybrids
31 hybrids

U3 hybrids
1,478 hybrids

non-U3 C/D box snoRNA hybrids
2,819 hybrids

B Conservation relative to flanking regions, split by proportion of hybrids conserved

100%,
265 interactions,
1,801 hybrids

>=50%,
20 interactions,
657 hybrids

<50%,
10 interactions,
160 hybrids

C Three snoRNA-EIF4A2 interactions that show a drop in conservation relative to flanking regions

SNORD2:::EIF4A2
42 hybrids

SNORD50B:::EIF4A2
5 hybrids

SNORD37:::EIF4A2
3 hybrids

D SNORD2 hybrid hits over EIF4A2 branch point region

Dunn-Davies et al. Fig. S6

A

Predicted snoRNA guided methylation sites on mRNAs (high confidence)

B

Predicted snoRNA guided methylation sites on mRNAs (potentially methylating)

Legend:
- Exon overlaps
- Host intron overlaps over branch point region
- Non-host intron overlaps outside branch point region
- Non-host intron overlaps over branch point region

Dunn-Davies et al. Fig. S7

A U3 3 days vs mock RNA-Seq results with all U3 targets highlighted.

count sig DE U3 targets: 231
count sig DE genes: 4657
proportion of U3 targets sig DE: 44%
proportion of genes sig DE: 29%
sig DE chisq pvalue: 3.44e-07

count sig upregulated U3 targets: 99
count sig upregulated genes: 2275
proportion of U3 targets sig upregulated: 19%
proportion of genes sig upregulated: 14%
sig upregulated chisq pvalue: 1.37e-02

count sig downregulated U3 targets: 132
count sig downregulated genes: 2382
proportion of U3 targets sig downregulated: 25%
proportion of genes sig downregulated: 15%
sig downregulated chisq pvalue: 1.62e-07

sig up vs down chisq pvalue: 8.69e-02

non-significant non-U3 target   non-significant U3 target   significant non-U3 target   significant U3 target

B U3 2 days vs mock RNA-Seq results with all U3 targets highlighted.

count sig DE U3 targets: 179
count sig DE genes: 3301
proportion of U3 targets sig DE: 35%
proportion of genes sig DE: 23%
sig DE chisq pvalue: 3.96e-06

count sig upregulated U3 targets: 78
count sig upregulated genes: 1601
proportion of U3 targets sig upregulated: 15%
proportion of genes sig upregulated: 11%
sig upregulated chisq pvalue: 1.68e-02

count sig downregulated U3 targets: 101
count sig downregulated genes: 1700
proportion of U3 targets sig downregulated: 20%
proportion of genes sig downregulated: 12%
sig downregulated chisq pvalue: 7.50e-06

sig up vs down chisq pvalue: 2.27e-01

non-significant non-U3 target   non-significant U3 target   significant non-U3 target   significant U3 target

Dunn-Davies et al. Fig. S8

Systematic mapping of small nucleolar RNA targets in human cells

Supplementary tables:

Table S1: Overall hybrid counts by biotype

Interaction	Total unfiltered hybrids	Filtered hybrids	Filters applied
snoRNA:::snoRNA	281,806	261,166	Reproducibility, Stability
lincRNA:::lincRNA	79,069	67,342	Reproducibility, Stability
snoRNA:::rRNA	73,374	57,069	Reproducibility, Stability, U3
mRNA:::mRNA	58,557	17,354	Reproducibility, Stability
snoRNA:::mRNA	52,819	7,209	Reproducibility, Stability, U3, rRNA
lincRNA:::mRNA	17,190	4,191	Reproducibility, Stability
lincRNA:::Mt-rRNA	4,461	3,012	Reproducibility, Stability
snoRNA:::lincRNA	4,277	676	Reproducibility, Stability, U3, rRNA
snoRNA:::Mt-rRNA	3,030	1,692	Reproducibility, Stability, U3, rRNA
Mt-rRNA:::Mt-rRNA	2,177	1,079	Reproducibility, Stability
misc-RNA:::misc-RNA	1,274	1,257	Reproducibility, Stability
mRNA:::Mt-rRNA	1,208	141	Reproducibility, Stability
snoRNA:::tRNA	947	591	Reproducibility, Stability, U3, rRNA
antisense:::antisense	925	672	Reproducibility, Stability
snoRNA:::snRNA	901	306	Reproducibility, Stability, U3, rRNA
lincRNA:::tRNA	860	454	Reproducibility, Stability
snoRNA:::antisense	739	100	Reproducibility, Stability, U3, rRNA
lincRNA:::Mt-tRNA	717	227	Reproducibility, Stability
snoRNA:::Mt-tRNA	677	385	Reproducibility, Stability, U3, rRNA
lincRNA:::snRNA	672	315	Reproducibility, Stability
snoRNA:::misc-RNA	643	418	Reproducibility, Stability, U3, rRNA
lincRNA:::misc-RNA	622	394	Reproducibility, Stability
antisense:::lincRNA	542	164	Reproducibility, Stability
processed-transcript:::processed-transcript	509	159	Reproducibility, Stability
antisense:::mRNA	471	45	Reproducibility, Stability
lincRNA:::processed-transcript	383	109	Reproducibility, Stability
snoRNA:::processed-transcript	339	65	Reproducibility, Stability, U3, rRNA
mRNA:::processed-transcript	309	33	Reproducibility, Stability
lincRNA:::rRNA	263	129	Reproducibility, Stability
mRNA:::tRNA	255	60	Reproducibility, Stability

Interaction	Total unfiltered hybrids	Filtered hybrids	Filters applied
mRNA:::Mt-tRNA	217	23	Reproducibility, Stability
misc-RNA:::mRNA	215	31	Reproducibility, Stability
mRNA:::snRNA	163	29	Reproducibility, Stability
Mt-rRNA:::Mt-tRNA	104	20	Reproducibility, Stability
lincRNA:::sense-overlapping	102	25	Reproducibility, Stability
lincRNA:::miRNA	90	21	Reproducibility, Stability
snoRNA:::sense-overlapping	85	20	Reproducibility, Stability, U3, rRNA
miRNA:::mRNA	79	13	Reproducibility, Stability
miRNA:::miRNA	59	52	Reproducibility, Stability
tRNA:::tRNA	57	32	Reproducibility, Stability
mRNA:::sense-overlapping	55	3	Reproducibility, Stability
mRNA:::rRNA	52	15	Reproducibility, Stability
Mt-rRNA:::tRNA	45	5	Reproducibility, Stability
Mt-tRNA:::Mt-tRNA	42	0	Reproducibility, Stability
Mt-rRNA:::processed-transcript	40	13	Reproducibility, Stability
antisense:::Mt-rRNA	38	6	Reproducibility, Stability
snoRNA:::miRNA	37	0	Reproducibility, Stability
misc-RNA:::Mt-rRNA	30	3	Reproducibility, Stability
snRNA:::snRNA	28	14	Reproducibility, Stability
snoRNA:::known-ncrna	27	2	Reproducibility, Stability, U3, rRNA
IG-C-gene:::mRNA	27	10	Reproducibility, Stability
known-ncrna:::lincRNA	25	18	Reproducibility, Stability
miRNA:::processed-transcript	25	3	Reproducibility, Stability
sense-overlapping::: sense-overlapping	23	3	Reproducibility, Stability
Mt-rRNA:::snRNA	20	2	Reproducibility, Stability
antisense:::processed-transcript	18	0	Reproducibility, Stability
antisense:::tRNA	14	0	Reproducibility, Stability
Mt-tRNA:::tRNA	14	3	Reproducibility, Stability
antisense:::misc-RNA	13	4	Reproducibility, Stability
lincRNA:::sense-intronic	11	5	Reproducibility, Stability
antisense:::Mt-tRNA	9	0	Reproducibility, Stability

Interaction	Total unfiltered hybrids	Filtered hybrids	Filters applied
Mt-rRNA:::sense-overlapping	9	2	Reproducibility, Stability
Mt-tRNA:::processed-transcript	9	0	Reproducibility, Stability
Mt-rRNA:::rRNA	9	2	Reproducibility, Stability
rRNA:::rRNA	8	6	Reproducibility, Stability
misc-RNA:::processed-transcript	7	0	Reproducibility, Stability
misc-RNA:::tRNA	7	0	Reproducibility, Stability
snoRNA:::IG-C-gene	7	0	Reproducibility, Stability
mRNA:::sense-intronic	7	1	Reproducibility, Stability
miRNA:::Mt-rRNA	6	3	Reproducibility, Stability
mRNA:::TEC	6	0	Reproducibility, Stability
antisense:::miRNA	6	0	Reproducibility, Stability
rRNA:::tRNA	6	0	Reproducibility, Stability
antisense:::rRNA	5	2	Reproducibility, Stability
IG-C-gene:::lincRNA	5	0	Reproducibility, Stability
processed-transcript:::tRNA	5	0	Reproducibility, Stability
Mt-rRNA:::sense-intronic	5	2	Reproducibility, Stability
antisense:::snRNA	5	0	Reproducibility, Stability
lincRNA:::TEC	4	0	Reproducibility, Stability
snoRNA:::TEC	4	0	Reproducibility, Stability
misc-RNA:::snRNA	4	0	Reproducibility, Stability
IG-C-gene:::IG-C-gene	4	4	Reproducibility, Stability
misc-RNA:::Mt-tRNA	4	2	Reproducibility, Stability
TEC:::TEC	4	0	Reproducibility, Stability
known-ncrna:::mRNA	4	0	Reproducibility, Stability
Mt-tRNA:::snRNA	3	0	Reproducibility, Stability
antisense:::TEC	3	0	Reproducibility, Stability
processed-transcript::: sense-overlapping	3	0	Reproducibility, Stability
sense-overlapping:::snRNA	3	0	Reproducibility, Stability
rRNA:::snRNA	3	0	Reproducibility, Stability
snRNA:::tRNA	2	0	Reproducibility, Stability
known-ncrna:::misc-RNA	2	0	Reproducibility, Stability

Interaction	Total unfiltered hybrids	Filtered hybrids	Filters applied
Mt-tRNA:::rRNA	2	0	Reproducibility, Stability
known-ncrna:::known-ncrna	2	0	Reproducibility, Stability
miRNA:::tRNA	2	0	Reproducibility, Stability
mRNA:::TR-C-gene	2	0	Reproducibility, Stability
antisense:::sense-overlapping	2	0	Reproducibility, Stability
IG-C-gene:::processed-transcript	1	0	Reproducibility, Stability
miRNA:::misc-RNA	1	0	Reproducibility, Stability
sense-overlapping:::tRNA	1	0	Reproducibility, Stability
snoRNA:::sense-intronic	1	0	Reproducibility, Stability
sense-intronic:::TEC	1	0	Reproducibility, Stability
known-ncrna:::tRNA	1	0	Reproducibility, Stability
miRNA:::Mt-tRNA	1	0	Reproducibility, Stability
mRNA:::non-coding	1	0	Reproducibility, Stability
3prime-overlapping-ncrna:::mRNA	1	0	Reproducibility, Stability

Table S2: High confidence methylating hybrids

Methylation site	snoRNA families	Box	Hybrid count	Source count	Category
28S-4588	SNORD91	(D' box)	1,994	16	Reported
18S-462	SNORD14	(D box)	670	12	Reported
18S-121	snoZ17	(D' box)	667	13	Reported
18S-27	SNORD27	(D' box)	653	9	Reported
28S-1858	SNORD38	(D' box)	435	11	Reported
18S-1490	SNORD25	(D' box)	427	10	Reported
18S-159	SNORD45	(D box)	417	10	Reported
18S-1288	SNORD110	(D' box)	416	13	Reported
18S-83	SNORD14	(D' box)	299	11	Not reported
18S-512	SNORD70	(D box)	277	12	Reported
18S-428	snoMBII-202	(D' box)	259	12	Reported
18S-1442	SNORD61	(D box)	257	9	Reported
18S-99	SNORD57	(D box)	218	9	Reported
28S-2338	SNORD24	(D box)	194	10	Reported
18S-627	SNORD65	(D' box)	194	9	Reported
18S-509	SNORD11B	(D box)	182	9	Reported
18S-668	SNORD36	(D box)	165	2	Reported
28S-2352	SNORD24	(D' box)	155	10	Reported
28S-4166	SNORD31	(D' box)	154	9	Reported
28S-2402	SNORD143, SNORD144	(D' box)	153	10	Reported
5.8S-75	SNORD96	(D box)	121	9	Reported
18S-116	SNORD42	(D box)	116	7	Reported
18S-1806	SNORD20	(D box)	110	9	Reported
18S-1705	SNORD43	(D' box)	91	3	Reported
18S-799	SNORD105, snoU105B	(D box)	86	9	Reported
28S-2774	SNORD99	(D box)	66	10	Reported
28S-2409	SNORD5	(D' box)	58	9	Reported
28S-4590	SNORD72	(D' box)	53	2	Reported
28S-391	SNORD81	(D' box)	42	9	Reported
18S-1031	SNORD59	(D' box)	41	2	Reported
28S-2411	snoZ40	(D' box)	36	6	Reported

Methylation site	snoRNA families	Box	Hybrid count	Source count	Category
18S-47	SNORD35	(D box)	34	2	Not reported
18S-172	SNORD45	(D' box)	33	8	Reported
28S-2802	SNORD95	(D box)	31	7	Reported
18S-1440	SNORD125	(D box)	30	8	Reported
28S-2811	SNORD95	(D' box)	30	7	Reported
28S-389	SNORD26	(D' box)	28	7	Reported
28S-1511	SNORD51, SNORD33	(D' box)	28	7	Reported
28S-2350	SNORD24	(D' box)	28	2	Reported
28S-1868	SNORD48	(D box)	23	8	Reported
28S-1313	SNORD18	(D' box)	21	4	Reported
28S-1327	SNORND104	(D' box)	17	5	Reported
28S-2824	SNORD34	(D' box)	17	5	Reported
18S-517	SNORD56	(D' box)	16	3	Reported
28S-4541	SNORD63	(D' box)	16	3	Reported
28S-3723	SNORD87	(D' box)	14	4	Reported
28S-3703	SNORD36	(D' box)	13	1	Reported
28S-4662	SNORD15	(D box)	9	1	Not reported
28S-3923	SNORD111	(D' box)	8	3	Reported
18S-683	SNORD19B	(D box)	8	2	Reported
28S-3697	SNORD37	(D' box)	8	2	Reported
18S-189	snoU83B	(D' box)	6	1	Not reported
28S-1310	SNORD126	(D' box)	5	2	Not reported
28S-3764	SNORD15	(D box)	5	4	Reported
18S-644	snoU54	(D box)	4	1	Reported
28S-4999	SNORD62	(D' box)	2	1	Not reported
18S-867	SNORD98	(D' box)	2	1	Reported
28S-3904	SNORD52	(D' box)	2	1	Reported
28S-879	SNORD73	(D' box)	1	1	Not reported
18S-174	SNORD45	(D' box)	1	1	Reported
28S-4522	SNORD63	(D box)	1	1	Reported

Table S3: Potentially methylating hybrids

Methylation site	snoRNA families	Box	Hybrid count	Source count	Category
28S-4588	SNORD91	(D' box)	1,799	15	Reported
18S-468	snoU83B	(D box)	904	14	Reported
18S-509	SNORD11, SNORD11B	(D box)	409	11	Reported
18S-412	U8	(D box)	401	12	Not reported
18S-116	SNORD42	(D box)	360	7	Reported
28S-1612	snosnR60_Z15	(D box)	243	10	Reported
28S-2848	SNORD50	(D box)	214	11	Reported
18S-484	SNORD16	(D' box)	212	7	Reported
18S-172	SNORD45	(D' box)	208	10	Reported
28S-1747	SNORD73	(D' box)	195	8	Reported
28S-4593	SNORD78	(D' box)	168	8	Reported
28S-3723	SNORD87	(D' box)	162	10	Reported
28S-15	SNORD47, SNORD91, SNORD36	(D box)	151	3	Not reported
28S-4506	SNORD35	(D' box)	136	9	Reported
18S-1605	U8, SNORD11B	(D box)	124	4	Not reported
28S-2863	SNORD50	(D' box)	124	10	Reported
18S-95	SNORD14	(D' box)	105	6	Not reported
28S-2388	snoMBII-202	(D box)	93	10	Reported
18S-436	SNORD100	(D' box)	74	9	Reported
18S-1452	snoU83B, SNORD51	(D box)	71	1	Not reported
18S-174	SNORD45	(D' box)	69	4	Reported
28S-20	SNORD43, SCARNA7	(D box)	67	1	Not reported
28S-21	snoR38, SNORD16	(D' box)	67	1	Not reported
18S-1272	SNORD66	(D' box)	64	6	Reported
28S-4581	SNORD78	(D box)	63	6	Not reported
18S-502	SNORD14	(D box)	49	6	Not reported
18S-507	snoU83B	(D box)	48	3	Not reported
18S-1164	SNORD2, SNORD70	(D' box)	41	5	Not reported
28S-1509	SNORD2	(D' box)	40	6	Reported
28S-30	SNORD43	(D' box)	37	1	Not reported

Methylation site	snoRNA families	Box	Hybrid count	Source count	Category
5.8S-14	SNORD71, SNORD21	(D' box)	37	6	Reported
28S-2435	SNORD2	(D' box)	35	5	Not reported
18S-601	SNORD103	(D' box)	34	5	Reported
18S-428	snoMBII-202	(D' box)	33	5	Reported
28S-1858	SNORD38	(D' box)	30	7	Reported
18S-854	SNORD53_SNORD92	(D box)	28	3	Not reported
18S-189	snoU83B	(D' box)	26	4	Not reported
18S-1433	SNORD74	(D' box)	25	2	Not reported
28S-17	SNORD77	(D box)	25	1	Not reported
18S-1610	SNORD50	(D' box)	24	1	Not reported
28S-4560	SNORD107	(D box)	24	5	Reported
18S-1425	SNORD74	(D box)	23	2	Not reported
28S-19	SNORD111	(D box)	23	1	Not reported
18S-1263	SNORD66	(D box)	22	5	Not reported
28S-56	SNORD12	(D box)	22	1	Not reported
18S-1391	SNORD28	(D box)	22	1	Reported
18S-405	SNORD100	(D box)	21	3	Not reported
18S-411	SNORD100	(D' box)	21	3	Not reported
18S-1615	SNORD110	(D' box)	21	3	Not reported
18S-1161	snoMBII-202	(D' box)	21	2	Not reported
28S-1456	U3	(D box)	18	4	Not reported
18S-1452	SNORD59, SNORD79	(D' box)	17	1	Not reported
28S-3031	U3	(D box)	16	4	Not reported
18S-157	SNORD65	(D' box)	16	1	Not reported
28S-4541	SNORD63	(D' box)	16	4	Reported
28S-2197	U3	(D box)	14	6	Not reported
28S-4586	SNORD37	(D box)	13	4	Not reported
18S-1605	SNORD12	(D' box)	13	2	Not reported
28S-22	snoR38	(D' box)	13	1	Not reported
28S-336	snoZ17	(D box)	13	1	Not reported
18S-668	SNORD36	(D box)	13	1	Reported
28S-4650	SNORD11B	(D box)	12	3	Not reported

9

Methylation site	snoRNA families	Box	Hybrid count	Source count	Category
18S-1170	snoU83B	(D box)	12	2	Not reported
28S-2347	SNORD70, SNORD27	(D box)	11	3	Not reported
28S-26	SNORD43	(D' box)	11	1	Not reported
18S-435	snoU83B	(D box)	10	2	Not reported
18S-21	SNORD53_SNORD92	(D' box)	10	1	Not reported
18S-504	SNORD56	(D box)	10	1	Not reported
28S-44	SNORD25	(D box)	10	1	Not reported
28S-54	SNORD38	(D' box)	10	1	Not reported
28S-4522	SNORD63	(D box)	10	4	Reported
18S-596	SNORD30	(D box)	9	3	Not reported
18S-115	SNORD31, SNORD22	(D box)	9	2	Not reported
18S-410	SNORD36	(D' box)	9	2	Not reported
18S-856	SNORD35	(D' box)	9	2	Not reported
28S-13	SNORD66	(D' box)	9	2	Not reported
18S-113	SNORD2	(D box)	9	1	Not reported
18S-1525	SNORD10	(D' box)	9	1	Not reported
28S-3697	SNORD37	(D' box)	9	3	Reported
18S-462	SNORD14	(D box)	9	2	Reported
18S-1490	SNORD25	(D' box)	9	2	Reported
28S-4592	SNORD57	(D' box)	8	4	Not reported
28S-2796	SNORD100	(D box)	8	2	Not reported
18S-127	SNORD43	(D' box)	8	1	Not reported
18S-1577	snoU13	(D box)	8	1	Not reported
18S-1739	SNORD103, SNORD36	(D' box)	8	1	Not reported
28S-14	SNORD50, SNORD86	(D box)	8	1	Not reported
18S-861	snoU83B	(D box)	7	4	Not reported
28S-1086	U3	(D box)	7	2	Not reported
28S-4649	SNORD11B	(D box)	7	2	Not reported
18S-10	SNORD25	(D box)	7	1	Not reported
18S-22	SNORD24	(D' box)	7	1	Not reported
18S-128	snoU83B	(D' box)	7	1	Not reported
18S-562	SNORD103	(D box)	7	1	Not reported

Methylation site	snoRNA families	Box	Hybrid count	Source count	Category
18S-993	SNORD59, SNORD30	(D' box)	7	1	Not reported
18S-1210	U8	(D box)	7	1	Not reported
18S-1510	SNORD58	(D' box)	7	1	Not reported
18S-1519	snoU83B	(D' box)	7	1	Not reported
28S-60	SNORD59	(D' box)	7	1	Not reported
28S-116	SNORD16	(D' box)	7	1	Not reported
18S-27	SNORD27	(D' box)	7	1	Reported
18S-34	SNORD28	(D' box)	7	1	Reported
18S-1163	SNORD90	(D box)	6	3	Not reported
28S-1716	SNORD39	(D' box)	6	3	Not reported
18S-126	SNORD96	(D box)	6	2	Not reported
18S-963	SNORD36	(D' box)	6	2	Not reported
18S-1512	SNORD14	(D box)	6	2	Not reported
18S-1822	snoU13	(D box)	6	2	Not reported
28S-4494	SNORD35	(D box)	6	2	Not reported
18S-409	snoZ17	(D box)	6	1	Not reported
18S-1201	SNORD110	(D' box)	6	1	Not reported
28S-2382	SNORD37	(D' box)	6	1	Not reported
28S-4964	SNORD107	(D' box)	6	1	Not reported
28S-5001	SNORD24	(D box)	6	1	Not reported
18S-517	SNORD56	(D' box)	6	1	Reported
18S-619	SNORD53_SNORD92	(D box)	5	2	Not reported
18S-1137	snoMBII-202	(D' box)	5	2	Not reported
28S-805	U3	(D box)	5	2	Not reported
18S-90	SNORD16	(D' box)	5	1	Not reported
18S-830	SNORD18	(D' box)	5	1	Not reported
18S-1598	SNORD33	(D box)	5	1	Not reported
18S-1702	SNORD65	(D box)	5	1	Not reported
18S-1730	SNORD65	(D' box)	5	1	Not reported
28S-13	SNORD66	(D box)	5	1	Not reported
28S-14	SNORD95	(D' box)	5	1	Not reported
28S-2333	SNORD24	(D' box)	4	3	Not reported

Methylation site	snoRNA families	Box	Hybrid count	Source count	Category
28S-2389	SNORD30	(D' box)	4	3	Not reported
28S-4044	U3	(D box)	4	2	Not reported
18S-79	SNORD70	(D box)	4	1	Not reported
18S-646	SNORD58	(D' box)	4	1	Not reported
18S-828	SNORD35	(D box)	4	1	Not reported
18S-1450	SNORD103	(D' box)	4	1	Not reported
18S-1473	SNORD2, SNORD51	(D' box)	4	1	Not reported
18S-1546	snoU54	(D box)	4	1	Not reported
18S-1674	SNORD110	(D' box)	4	1	Not reported
28S-723	snoU83B	(D box)	4	1	Not reported
28S-1604	SNORD83	(D box)	4	1	Not reported
28S-2414	SNORD2	(D box)	4	1	Not reported
28S-2430	SNORD58	(D' box)	4	1	Not reported
28S-2502	SNORD81, SNORD26	(D' box)	4	1	Not reported
28S-2514	SNORD69, SNORD57	(D' box)	4	1	Not reported
28S-4718	SNORD39	(D box)	4	1	Not reported
28S-5026	snoU54	(D' box)	4	1	Not reported
18S-121	SNORND104	(D box)	4	2	Reported
18S-683	SNORD19	(D box)	4	2	Reported
18S-1031	SNORD59	(D' box)	4	1	Reported
18S-599	snoU83B	(D box)	3	2	Not reported
28S-2413	snoMBII-202	(D' box)	3	2	Not reported
28S-4767	U3	(D box)	3	2	Not reported
18S-43	SNORD42	(D' box)	3	1	Not reported
18S-84	SNORD59, SNORD126	(D' box)	3	1	Not reported
18S-104	SNORD19	(D' box)	3	1	Not reported
18S-114	SNORD79	(D' box)	3	1	Not reported
18S-421	SNORD58	(D' box)	3	1	Not reported
18S-1285	SNORD69	(D box)	3	1	Not reported
18S-1421	SNORD44	(D box)	3	1	Not reported
18S-1430	SNORD44	(D' box)	3	1	Not reported
18S-1435	SNORD43	(D' box)	3	1	Not reported

Methylation site	snoRNA families	Box	Hybrid count	Source count	Category
18S-1449	SNORD60	(D' box)	3	1	Not reported
18S-1485	SNORD34	(D' box)	3	1	Not reported
18S-1731	SNORD30	(D box)	3	1	Not reported
18S-1735	SNORD103	(D box)	3	1	Not reported
ITS2-461	SNORD12	(D' box)	3	1	Not reported
28S-2221	U3	(D box)	3	1	Not reported
28S-2226	U3	(D box)	3	1	Not reported
28S-2496	SNORD83	(D' box)	3	1	Not reported
28S-2807	SNORD28	(D box)	3	1	Not reported
28S-2903	SNORD31	(D' box)	3	1	Not reported
28S-4607	SNORD121A	(D' box)	3	2	Reported
18S-99	SNORD57	(D box)	3	1	Reported
18S-683	SNORD19B	(D' box)	3	1	Reported
18S-118	SNORND104	(D box)	2	2	Not reported
28S-554	U3	(D box)	2	2	Not reported
28S-2898	SNORD29	(D' box)	2	2	Not reported
18S-130	SNORD2	(D' box)	2	1	Not reported
18S-144	SNORND104	(D' box)	2	1	Not reported
18S-389	snoU6-53	(D' box)	2	1	Not reported
18S-416	SNORD65	(D box)	2	1	Not reported
18S-591	SNORD42	(D box)	2	1	Not reported
18S-612	SNORD43, SNORD41	(D box)	2	1	Not reported
18S-613	SNORD58	(D' box)	2	1	Not reported
18S-796	SNORD25	(D' box)	2	1	Not reported
18S-806	SNORD83	(D' box)	2	1	Not reported
18S-817	SNORD2	(D box)	2	1	Not reported
18S-836	SNORD2	(D' box)	2	1	Not reported
18S-980	SNORD16	(D' box)	2	1	Not reported
18S-1012	SNORD103	(D box)	2	1	Not reported
18S-1048	SNORD50	(D' box)	2	1	Not reported
18S-1128	SNORD50	(D box)	2	1	Not reported
18S-1140	SNORD50	(D' box)	2	1	Not reported

Methylation site	snoRNA families	Box	Hybrid count	Source count	Category
18S-1199	snoU83B	(D box)	2	1	Not reported
18S-1261	SNORD65	(D box)	2	1	Not reported
18S-1284	SNORD38	(D' box)	2	1	Not reported
18S-1289	SNORD20	(D box)	2	1	Not reported
18S-1412	U3	(D box)	2	1	Not reported
18S-1477	SNORD42, SNORD110	(D' box)	2	1	Not reported
18S-1518	SNORD48	(D box)	2	1	Not reported
18S-1520	SNORD91	(D box)	2	1	Not reported
18S-1549	SNORD126	(D box)	2	1	Not reported
18S-1570	SNORD126	(D' box)	2	1	Not reported
18S-1571	snoZ40	(D box)	2	1	Not reported
18S-1584	snoZ40	(D' box)	2	1	Not reported
18S-1596	SNORD142;ZL68	(D' box)	2	1	Not reported
18S-1737	SNORD82	(D' box)	2	1	Not reported
18S-1738	SNORD100, SNORD36	(D' box)	2	1	Not reported
18S-1857	SNORD50	(D' box)	2	1	Not reported
5.8S-12	SNORD36	(D box)	2	1	Not reported
5.8S-136	snoU83B	(D' box)	2	1	Not reported
28S-2	SNORD166	(D box)	2	1	Not reported
28S-53	SNORD125	(D box)	2	1	Not reported
28S-57	snoU105B	(D' box)	2	1	Not reported
28S-1362	SNORD65	(D box)	2	1	Not reported
28S-1382	SNORD65	(D' box)	2	1	Not reported
28S-2394	SNORD62	(D' box)	2	1	Not reported
28S-2699	SNORD31	(D' box)	2	1	Not reported
28S-2739	SNORD12	(D' box)	2	1	Not reported
28S-2823	SNORD103	(D box)	2	1	Not reported
28S-2871	snoR38	(D box)	2	1	Not reported
28S-3596	SNORD18	(D' box)	2	1	Not reported
28S-4630	SNORD73	(D' box)	2	1	Not reported
18S-121	snoZ17, SNORD71	(D' box)	2	2	Reported
28S-2802	SNORD95	(D box)	2	2	Reported

Methylation site	snoRNA families	Box	Hybrid count	Source count	Category
18S-627	SNORD65	(D' box)	2	1	Reported
18S-866	SNORD34	(D' box)	2	1	Reported
5.8S-14	SNORD34	(D box)	2	1	Reported
5.8S-69	SNORD31	(D box)	2	1	Reported
28S-2409	SNORD53_SNORD92	(D' box)	2	1	Reported
18S-43	snoR38	(D box)	1	1	Not reported
18S-47	SNORD35	(D box)	1	1	Not reported
18S-70	snoR38	(D' box)	1	1	Not reported
18S-83	SNORD14	(D' box)	1	1	Not reported
18S-102	SNORD36	(D box)	1	1	Not reported
18S-110	SNORD135;ZL2	(D box)	1	1	Not reported
18S-113	SNORD27	(D' box)	1	1	Not reported
18S-114	snoR38	(D box)	1	1	Not reported
18S-127	U3	(D box)	1	1	Not reported
18S-205	SNORD36	(D' box)	1	1	Not reported
18S-379	SNORND104	(D' box)	1	1	Not reported
18S-396	SNORD65	(D' box)	1	1	Not reported
18S-408	SNORD48	(D' box)	1	1	Not reported
18S-411	U8	(D box)	1	1	Not reported
18S-417	SNORD30	(D box)	1	1	Not reported
18S-430	SNORND104	(D box)	1	1	Not reported
18S-433	SNORD30	(D' box)	1	1	Not reported
18S-441	SNORD35	(D' box)	1	1	Not reported
18S-443	snoU83B	(D' box)	1	1	Not reported
18S-451	SNORD95	(D box)	1	1	Not reported
18S-453	SNORND104	(D' box)	1	1	Not reported
18S-461	SNORD42	(D box)	1	1	Not reported
18S-467	SNORD38	(D box)	1	1	Not reported
18S-471	snoZ40	(D box)	1	1	Not reported
18S-476	SNORD38	(D' box)	1	1	Not reported
18S-477	snoZ40	(D' box)	1	1	Not reported
18S-515	SNORD2	(D box)	1	1	Not reported

Methylation site	snoRNA families	Box	Hybrid count	Source count	Category
18S-592	SNORD35	(D' box)	1	1	Not reported
18S-599	SNORD14	(D' box)	1	1	Not reported
18S-600	U8	(D box)	1	1	Not reported
18S-613	SNORD172;ZL24	(D box)	1	1	Not reported
18S-617	SNORD30	(D' box)	1	1	Not reported
18S-621	snoZ17	(D box)	1	1	Not reported
18S-623	SNORD30	(D' box)	1	1	Not reported
18S-702	SNORD19	(D' box)	1	1	Not reported
18S-788	snoU13	(D' box)	1	1	Not reported
18S-818	SNORD44	(D box)	1	1	Not reported
18S-819	SNORD60	(D' box)	1	1	Not reported
18S-827	SNORD95	(D box)	1	1	Not reported
18S-829	SNORD44	(D' box)	1	1	Not reported
18S-893	SNORD63	(D box)	1	1	Not reported
18S-961	SNORD58	(D' box)	1	1	Not reported
18S-969	SNORD59	(D box)	1	1	Not reported
18S-972	snoU83B	(D box)	1	1	Not reported
18S-983	SNORD18	(D' box)	1	1	Not reported
18S-1052	SNORD59	(D' box)	1	1	Not reported
18S-1163	SNORD83	(D' box)	1	1	Not reported
18S-1166	snoU83B	(D box)	1	1	Not reported
18S-1168	SNORD36	(D' box)	1	1	Not reported
18S-1184	snoU13	(D' box)	1	1	Not reported
18S-1229	SNORD67	(D' box)	1	1	Not reported
18S-1231	SNORD48	(D box)	1	1	Not reported
18S-1274	SNORD50	(D' box)	1	1	Not reported
18S-1423	U3	(D box)	1	1	Not reported
18S-1441	SNORD42	(D box)	1	1	Not reported
18S-1453	SNORD124	(D box)	1	1	Not reported
18S-1511	snoMBII-202	(D' box)	1	1	Not reported
18S-1546	snoU13	(D' box)	1	1	Not reported
18S-1573	SNORD110	(D box)	1	1	Not reported

Methylation site	snoRNA families	Box	Hybrid count	Source count	Category
18S-1574	snoZ17	(D box)	1	1	Not reported
18S-1575	snoR38	(D' box)	1	1	Not reported
18S-1616	SNORD59	(D box)	1	1	Not reported
18S-1667	SNORD35	(D box)	1	1	Not reported
18S-1706	SNORD35	(D' box)	1	1	Not reported
18S-1725	snoU13	(D' box)	1	1	Not reported
18S-1730	SNORD67	(D box)	1	1	Not reported
18S-1733	SNORD57	(D box)	1	1	Not reported
18S-1734	SNORD100	(D box)	1	1	Not reported
18S-1736	SNORD2	(D box)	1	1	Not reported
18S-1740	SNORD43	(D' box)	1	1	Not reported
18S-1758	SNORD133;ZL142	(D box)	1	1	Not reported
5.8S-29	SNORD27	(D' box)	1	1	Not reported
5.8S-41	SNORD36	(D' box)	1	1	Not reported
5.8S-50	SNORND104	(D' box)	1	1	Not reported
5.8S-108	SNORD38	(D box)	1	1	Not reported
5.8S-114	SNORD38	(D' box)	1	1	Not reported
5.8S-116	SNORD65	(D box)	1	1	Not reported
28S-23	SNORD49	(D' box)	1	1	Not reported
28S-28	SNORD88	(D' box)	1	1	Not reported
28S-29	SNORD166	(D' box)	1	1	Not reported
28S-69	SNORD12	(D box)	1	1	Not reported
28S-75	snoR38	(D box)	1	1	Not reported
28S-103	snoR38	(D' box)	1	1	Not reported
28S-208	SNORD47	(D box)	1	1	Not reported
28S-378	SNORD111	(D' box)	1	1	Not reported
28S-383	SNORD26	(D box)	1	1	Not reported
28S-1419	SNORD2	(D' box)	1	1	Not reported
28S-1576	SNORND104	(D' box)	1	1	Not reported
28S-1722	SNORD65	(D' box)	1	1	Not reported
28S-1726	SNORD25	(D' box)	1	1	Not reported
28S-1831	SNORD103	(D box)	1	1	Not reported

Methylation site	snoRNA families	Box	Hybrid count	Source count	Category
28S-1932	SNORD60	(D' box)	1	1	Not reported
28S-2215	U3	(D box)	1	1	Not reported
28S-2330	SNORD33	(D box)	1	1	Not reported
28S-2335	SNORD24	(D box)	1	1	Not reported
28S-2344	SNORD24	(D' box)	1	1	Not reported
28S-2367	SNORD33	(D' box)	1	1	Not reported
28S-2379	SNORD65	(D box)	1	1	Not reported
28S-2382	SNORD12	(D box)	1	1	Not reported
28S-2391	SNORD30	(D' box)	1	1	Not reported
28S-2392	SNORD51	(D box)	1	1	Not reported
28S-2410	SNORD36	(D box)	1	1	Not reported
28S-2416	SNORD30	(D' box)	1	1	Not reported
28S-2492	SNORD50	(D box)	1	1	Not reported
28S-2828	SNORD60	(D' box)	1	1	Not reported
28S-2831	SNORD27	(D box)	1	1	Not reported
28S-2844	SNORD16	(D' box)	1	1	Not reported
28S-2887	SNORD50	(D box)	1	1	Not reported
28S-2897	SNORD50	(D' box)	1	1	Not reported
28S-3446	U3	(D box)	1	1	Not reported
28S-3584	SNORD14	(D box)	1	1	Not reported
28S-3615	SNORD35	(D' box)	1	1	Not reported
28S-3626	SNORD51	(D box)	1	1	Not reported
28S-3641	snoU83B	(D box)	1	1	Not reported
28S-3659	snoU83B	(D' box)	1	1	Not reported
28S-3734	U8	(D box)	1	1	Not reported
28S-4459	snoU13	(D' box)	1	1	Not reported
28S-4486	SNORD14	(D' box)	1	1	Not reported
28S-4495	SNORD35	(D' box)	1	1	Not reported
28S-4499	SNORD91	(D' box)	1	1	Not reported
28S-4572	SNORD30	(D' box)	1	1	Not reported
28S-4576	SNORD100	(D' box)	1	1	Not reported
28S-4589	SNORD121A	(D box)	1	1	Not reported

Methylation site	snoRNA families	Box	Hybrid count	Source count	Category
28S-4596	SNORD110	(D box)	1	1	Not reported
28S-4603	SNORD105	(D' box)	1	1	Not reported
28S-4652	snoZ17	(D box)	1	1	Not reported
28S-4849	SNORD58	(D' box)	1	1	Not reported
28S-4958	SNORD25	(D' box)	1	1	Not reported
28S-4979	SNORD38	(D' box)	1	1	Not reported
28S-4994	SNORD48	(D box)	1	1	Not reported
28S-4996	snoU54	(D box)	1	1	Not reported
28S-4996	SNORD30	(D' box)	1	1	Not reported
28S-5003	SNORD96	(D' box)	1	1	Not reported
18S-27	SNORD15	(D box)	1	1	Reported
18S-644	snoU54	(D box)	1	1	Reported
18S-867	SNORD98	(D' box)	1	1	Reported
18S-1172	SNORD31	(D box)	1	1	Reported
18S-1288	SNORD110	(D' box)	1	1	Reported
18S-1447	snoU89	(D box)	1	1	Reported
18S-1536	snoU89	(D box)	1	1	Reported
18S-1668	SNORD67	(D box)	1	1	Reported
18S-1668	SNORD94	(D' box)	1	1	Reported
28S-389	SNORD26	(D' box)	1	1	Reported
28S-2791	SNORD35	(D' box)	1	1	Reported
28S-3764	SNORD15	(D box)	1	1	Reported
28S-4032	SNORD75	(D' box)	1	1	Reported

Table S4: Ancillary hybrid counts

Interaction	Hybrid count	Experiment count
SNORD25 : 18S-10	35	2
SNORD31 : 5.8S-69	23	1
SNORD48 : 18S-1518	19	1
SNORD59 : 28S-60	19	1
SNORD2 : 18S-113	17	1
SNORD58 : 18S-421	17	1
SNORD20 : 18S-1804	16	3
SNORD20 : 18S-1806	16	3
SNORD35 : 28S-2791	16	2
SNORD100 : 18S-436	13	1
SNORD110 : 18S-1477	13	3
SNORD110 : 18S-1573	13	3
SNORD126 : 18S-84	13	1
SNORD2 : 18S-1736	13	1
snoU83B : 18S-1519	13	1
SNORD103 : 18S-1668	12	1
U8 : 18S-1210	12	1
snoU83B : 28S-3659	12	1
SNORD25 : 28S-44	11	1
snoZ17 : 18S-409	10	2
snoU83B : 28S-3641	10	1
SNORD35 : 18S-441	9	1
SNORD35 : 18S-856	9	4
U3 : 28S-3031	9	3
SNORD30 : 18S-1731	8	1
SNORD33 : 18S-1326	8	3
SNORD24 : 18S-22	8	1
snoU83B : 18S-1199	8	1
SNORD103 : 18S-1739	8	1
SNORD11B : 18S-1605	7	2
SNORD16 : 28S-2844	7	1

Interaction	Hybrid count	Experiment count
SNORD35 : 18S-1667	7	1
SNORD37 : 28S-3697	7	1
SNORD48 : 18S-1231	7	2
SNORD65 : 18S-157	7	1
SNORD2 : 18S-130	6	1
SNORD31 : 28S-2903	6	1
SNORD43 : 18S-127	6	1
SNORD69 : 18S-1285	6	1
snoU83B : 18S-128	6	3
SNORD100 : 28S-4576	5	1
U8 : 18S-411	5	1
U8 : 18S-412	5	1
U8 : 18S-1605	5	1
SNORD14 : 18S-1512	5	1
SNORD33 : 18S-1328	5	1
SNORD57 : 18S-99	5	1
SNORD70 : 18S-79	5	1
SNORD79 : 18S-114	5	1
snoU83B : 18S-507	5	1
snoU83B : 18S-599	5	1
SNORD103 : 28S-2823	5	1
SNORD142;ZL68 : 18S-1596	4	2
SNORD36 : 28S-15	4	1
SNORD38 : 18S-467	4	1
SNORD38 : 18S-476	4	1
SNORD44 : 18S-818	4	1
SNORD44 : 18S-829	4	1
snoZ17 : 18S-1574	4	1
SNORD58 : 18S-1510	4	1
SNORND104 : 18S-144	3	1
SNORND104 : 5.8S-50	3	1
SNORD110 : 18S-1674	3	2

Interaction	Hybrid count	Experiment count
snoR38 : 18S-70	3	1
SNORD27 : 28S-2347	3	1
SNORD30 : 18S-417	3	1
SNORD30 : 18S-433	3	1
SNORD36 : 18S-1739	3	1
SNORD42 : 18S-43	3	1
SNORD45 : 18S-159	3	1
SNORD58 : 18S-613	3	1
SNORD59 : 18S-84	3	1
snoZ40 : 18S-1571	3	1
SNORD62 : 28S-2394	3	2
SNORD63 : 18S-893	3	1
SNORD66 : 28S-13	3	2
snoMBII-202 : 18S-1511	3	1
SNORA46 : 18S-649	2	1
SNORD100 : 18S-405	2	1
SNORD100 : 18S-411	2	1
SNORND104 : 28S-1576	2	1
snoU105B : 28S-57	2	1
SNORD12 : 28S-2739	2	1
snoU13 : 18S-1725	2	1
SNORD133;ZL142 : 18S-1758	2	1
SNORD135;ZL2 : 18S-110	2	1
SNORD15 : 18S-27	2	1
SNORD19 : 18S-702	2	1
snoR38 : 28S-2871	2	1
SNORD2 : 18S-1164	2	1
SNORD31 : 18S-1172	2	1
SNORD33 : 18S-1598	2	1
SNORD34 : 18S-1485	2	1
SNORD34 : 5.8S-14	2	1
SNORD35 : 18S-47	2	2

Interaction	Hybrid count	Experiment count
SNORD35 : 18S-828	2	1
SNORD36 : 28S-3703	2	1
SNORD36 : 18S-410	2	1
SNORD36 : 18S-668	2	1
SNORD38 : 28S-4979	2	2
U3 : 28S-3446	2	2
SNORD42 : 18S-461	2	1
snoZ17 : 18S-121	2	1
SNORD39 : 28S-2791	2	1
SNORD59 : 18S-1616	2	1
snoZ40 : 18S-1584	2	1
SNORD65 : 18S-396	2	1
SNORD65 : 18S-1261	2	1
SNORD65 : 28S-1722	2	1
SNORD83 : 18S-806	2	1
SNORD86 : 18S-1219	2	2
SNORD100 : 18S-1734	1	1
SNORD100 : 18S-1738	1	1
U8 : 18S-600	1	1
SNORD12 : 18S-1536	1	1
SNORD14 : 18S-462	1	1
snoR38 : 18S-114	1	1
snoR38 : 18S-1575	1	1
snoR38 : 18S-43	1	1
SNORD25 : 18S-1490	1	1
SNORD30 : 18S-1383	1	1
SNORD36 : 18S-205	1	1
SNORD36 : 18S-1738	1	1
SNORD45 : 18S-159	1	1
SNORD65 : 18S-416	1	1
snoMBII-202 : 18S-428	1	1
SNORD73 : 28S-1747	1	1

Interaction	Hybrid count	Experiment count
snoU83B : 18S-1199	1	1
SNORD91 : 28S-4588	1	1
SNORD53_SNORD92 : 18S-619	1	1

Table S5: Blocking hybrid counts

Interaction	Hybrid count	Experiment count
snoZ17 : 28S-4589	9	1
snoZ17 : 28S-4588	8	1
SNORD91 : 18S-1052	8	2
snoZ17 : 28S-4592	4	1
snoZ17 : 28S-4593	4	1
SCARNA17 : 18S-93	3	1
SNORD33 : 18S-93	1	1
SNORD91 : 18S-1056	4	1
snoZ17 : 28S-4596	3	1
snoZ17 : 28S-4598	3	1
SCARNA17 : 18S-95	2	1
SNORD33 : 18S-95	1	1
SNORD34 : 18S-22	2	1
SNORD34 : 18S-27	2	1
SNORD34 : 18S-28	2	1
SCARNA17 : 18S-90	1	1
SNORD33 : 18S-90	1	1
snoZ17 : 28S-4590	1	1
snoZ17 : 28S-4603	1	1
SNORD34 : 18S-21	1	1
SNORD33 : 18S-84	1	1

Table S6: Structural hybrid counts

Interaction	Hybrid count	Experiment count
U3	6,827	14
U8	2,118	12
snoU83B	1,124	11
SNORD58	1,022	3
SNORD14	834	11
snoU13	812	13
SNORD62	580	7
SNORD38	543	6
SNORD91	501	4
snoR38	472	4
SNORD103	429	4
SNORD44	419	1
SNORD83	416	5
SNORD107	396	2
SNORD100	394	7
SNORD36	380	3
SNORD110	342	7
SNORD34	321	3
SNORD2	310	2
snoZ17	307	3
SNORD16	301	6
SNORD45	295	3
snoMBII-202	294	6
SNORD31	255	5
snoU2_19	251	5
others	8,057	16